

## **Intracrine endothelin signalling evokes IP3-dependent increases in nucleoplasmic Ca<sup>2+</sup> in adult cardiac myocytes\***

Clémence Merlen<sup>a,b</sup>, Nada Farhat<sup>a</sup>, Xiaoyan Luo<sup>a,c</sup>, David Chatenet<sup>f</sup>, Artavazd Tadevosyan<sup>a,c</sup>, Louis R. Villeneuve<sup>a</sup>, Marc-Antoine Gillis<sup>a</sup>, Stanley Nattel<sup>a,d,g</sup>, Eric Thorin<sup>a,b,e</sup>, Alain Fournier<sup>f</sup>, and Bruce G. Allen<sup>a,b,d,g</sup>

From <sup>a</sup>Montreal Heart Institute, and the Departments of <sup>b</sup>Biochemistry, <sup>c</sup>Biomedical Sciences, <sup>d</sup>Medicine, and <sup>e</sup>Surgery, Université de Montréal, Montréal, Québec, H3C 3J7, Canada. <sup>f</sup>Institut Armand-Frappier, Institut national de la recherche scientifique, Université du Québec, 531 boul. des Prairies, Laval, Québec H7V 1B7, Canada. <sup>g</sup>Department of Pharmacology and Therapeutics, McGill University, Montréal, Québec, H3G 1Y6, Canada.

Address correspondence to:

Bruce G. Allen

Montreal Heart Institute

5000 Belanger St.

Montréal, Québec, Canada

HIT 1C8.

Telephone: (514) 376-3330 (3591).

FAX: (514) 376-1355.

E-mail: [bruce.g.allen@umontreal.ca](mailto:bruce.g.allen@umontreal.ca)

Running head: Nuclear ETB receptors

## **Abstract**

Endothelin receptors are present on the nuclear membranes in adult cardiac ventricular myocytes. The objectives of the present study were to determine 1) which endothelin receptor subtype is in cardiac nuclear membranes, 2) if the receptor and ligand traffic from the cell surface to the nucleus, and 3) the effect of increased intracellular ET-1 on nuclear  $Ca^{2+}$  signalling. Confocal microscopy using fluorescently-labeled endothelin analogs confirmed the presence of ETB at the nuclear membrane of rat cardiomyocytes in skinned-cells and isolated nuclei. Furthermore, in both cardiac myocytes and aortic endothelial cells, endocytosed ET:ETB complexes translocated to lysosomes and not the nuclear envelope. Although ETA and ETB can form heterodimers, the presence or absence of ETA did not alter ETB trafficking. Treatment of isolated nuclei with peptide: N-glycosidase F did not alter the electrophoretic mobility of ETB. The absence of N-glycosylation further indicating that these receptors did not originate at the cell surface. Intracellular photolysis of a caged ET-1 analog ([Trp-ODMNB<sup>21</sup>]ET-1) evoked an increase in nucleoplasmic  $Ca^{2+}$  ( $[Ca^{2+}]_n$ ) that was attenuated by the inositol 1,4,5-trisphosphate receptor inhibitor 2-aminoethoxydiphenyl borate and prevented by pre-treatment with ryanodine. A caged cell-permeable analog of the ETB-selective antagonist IRL-2500 blocked the ability of intracellular cET-1 to increase  $[Ca^{2+}]_n$  whereas extracellular application of ETA and ETB receptor antagonists did not. These data suggest that 1) the endothelin receptor in the cardiac nuclear membranes is ETB, 2) ETB traffic directly to the nuclear membrane after biosynthesis, 3) exogenous endothelins are not ligands for ETB on nuclear membranes, and 4) ETB associated with the nuclear membranes regulate nuclear  $Ca^{2+}$  signalling.

**Keywords:** endothelin receptor, nuclear envelope, nuclear  $Ca^{2+}$ , receptor trafficking, stimulus-transcription coupling

## 1. Introduction

The endothelins (ETs) comprise three isopeptides (ET-1, ET-2, ET-3), each arising from a separate gene. The actions of endothelins are mediated by two receptor subtypes, ETA and ETB, which couple to multiple signalling systems [1]. ETA and ETB receptors bind the three ETs with differing affinities: ETA has greater affinity for ET-1 and ET-2 than ET-3, while ETB binds all endothelin peptides with equal affinity [2, 3]. In heterologous expression systems, ETA and ETB differ in their internalization and intracellular trafficking. ETA shows ligand-dependent endocytosis and is recycled back to the plasma membrane whereas ETB internalizes constitutively and translocate to lysosomes [4-6]. Thus, it has been proposed that ETA, the prevalent receptor subtype in the cardiac tissue, mediates the main cellular functions of endothelin, whereas ETB is involved in the clearance of ET-1. However, since ET-3 also evokes a hypertrophic response [7] and the pathogenic effects of conditional, myocyte-specific ET-1 overexpression are delayed by a mixed ETA/ETB antagonist but not an ETA-selective antagonist [8], ETB also plays an important functional role in adult cardiac ventricular myocytes.

To date, the cellular signalling events initiated by ET-1 have been best characterized for endothelin receptors at the cell surface. However, endothelin receptors, as well as several other GPCRs and their effectors, are also present on cardiac nuclear membranes (reviewed in [9-11]). Immunocytofluorescence studies have revealed ETA to be primarily in the plasma membrane with some perinuclear staining, whereas ETB localize to the nuclear membrane in ventricular myocytes [12, 13]. The presence of GPCR effector molecules at the nuclear envelope or within the nucleus further supports the concept of GPCR signalling at the nuclear membrane [14]. In human vascular smooth muscle cells, the cytosolic application of ET-1 induces an increase of nuclear  $Ca^{2+}$  [15]. Furthermore, direct stimulation of isolated cardiac nuclei with ET-1 induces a transient increase in luminal  $Ca^{2+}$ , activates endogenous nuclear protein kinase activities [12], and reduces *de novo* RNA synthesis [16]. In contrast, treatment of isolated cardiac nuclei with

isoproterenol or angiotensin II (Ang II) increases transcription initiation [16-18]. Similarly, dynorphin B, an agonist of the  $\kappa$  opioid receptor, increases opioid peptide transcription in isolated cardiac nuclei [19]. In nuclei isolated from non-cardiac cells, Ang II [20], bradykinin B2 [21], prostaglandin E<sub>2</sub> [22-24], lysophosphatidic acid type-1 [25, 26], metabotropic glutamate type-5 [27, 28], thromboxane A2 [29, 30], and urotensin-II [31] receptor activation also altered gene expression. Hence, endothelin receptors couple to effectors within the nuclear membrane and may be involved in stimulus-transcription coupling. In the present study, we now show that the endothelin receptors in cardiac nuclear membranes are of the ETB subtype. We also demonstrate that nuclear ETB is not derived from the cell surface and, similarly, these receptors are not regulated by ligand taken up from the extracellular media. Furthermore, the intracellular release of a caged ET-1 analog in ventricular myocytes resulted in an inositol 1,4,5-trisphosphate receptor (IP3R)-mediated increase in nucleoplasmic [Ca<sup>2+</sup>] and an activation of CaMKII. This increase in nucleoplasmic [Ca<sup>2+</sup>] was inhibited by a cell-permeable analog of the ETB-selective antagonist IRL2500 but not by extracellular application of ETA and ETB antagonists.

## **2. Materials and Methods**

### *2.1. Materials*

FAM-ET-1, rhodamine-ET-1, and LysoTracker were from Phoenix Pharmaceuticals, Inc. Anti-ETB and anti-ETA antibodies were from Alomone. Anti-importin  $\beta$  antibodies and Protein A/G PLUS-Agarose were from Santa Cruz Biotechnology, Inc. HRP-conjugated secondary antibodies were from Jackson ImmunoResearch Laboratories. Alexa Fluor 488-conjugated donkey anti-rabbit IgG and Alexa Fluor 555-conjugated donkey anti-goat IgG were from Molecular Probes. Electrophoresis and immunoblotting reagents were from Bio-Rad Laboratories.

### *2.2. Isolation of cardiac ventricular myocytes*

Calcium-tolerant cardiomyocytes were isolated as described previously [32]. All animal handling procedures were approved by the Animal Research Ethics Committee of the Montreal Heart Institute and the procedures complied with guidelines established in the Guide for the Care and Use of Laboratory Animals (NIH Publication 65-23, revised 1996).

### *2.3. Isolation of nuclei from cardiac ventricular myocytes*

Nuclei were isolated from freshly isolated adult rat cardiac ventricular myocytes as described previously [33, 34]. Briefly, following isolation, ventricular myocytes were resuspended in PBS and centrifuged at 200  $\times g$  for 10 min at room temperature. Cells were then resuspended in buffer 1 (10 mM HEPES pH 7.4, 320 mM sucrose, 5 mM MgCl<sub>2</sub>, 1 mM DTT, and 1 mM PMSF) containing 1% (v/v) Triton X-100. Cells were sonicated for 40 s then maintained on ice for 10 min. Nuclei were isolated by centrifugation for 15 min at 18 000  $\times g$  and 4°C into a discontinuous sucrose density gradient in buffer 2 (10 mM HEPES pH 7.4, 1.8 M sucrose, 5 mM MgCl<sub>2</sub>, 1 mM DTT, and 1 mM PMSF). The pellet containing the nuclear fraction was resuspended in buffer 1.

#### 2.4. *Isolation of endothelial cells*

Rat aortic endothelial cells were isolated by an explant technique [35]. Briefly, six to eight 1-mm<sup>2</sup> segments of artery were seeded in 35 mm<sup>2</sup> culture dishes to obtain five to eight segments anchored on Matrigel. Cells were incubated in Dulbecco's Modified Eagle Medium (DMEM) supplemented with 10% foetal bovine serum, 10% calf serum, 1% penicillin-streptomycin, 90 µg/ml sodium heparin salt, 60 mg/ml EC growth supplement, and 100 U/ml fungizone, at 37°C in a 95% air and 5% CO<sub>2</sub> incubator. Passage 2 cells were used.

Porcine aortic endothelial cells were isolated by enzymatic digestion using type II collagenase as described previously [36]. Cells were grown in Dulbecco's Modified Eagle Medium (DMEM) supplemented with 10% foetal bovine serum, 1% penicillin-streptomycin, and glutamine. When 90% confluence was reached, the buffer was replaced with DMEM containing penicillin-streptomycin and glutamine, without serum (starving medium). After 16 h, the starving medium was replaced and cells were employed for immunocytofluorescence. Cells were passaged once.

#### 2.5. *Isolation of nuclei from rat heart*

Nuclei were isolated from rat heart as described previously [12, 17, 18].

#### 2.6. *Immunoprecipitation*

Immunoprecipitation assays were performed on whole cell lysates (500 µg) extracted from porcine aortic endothelial cells or from rat heart nuclei. Samples were incubated with an anti-importin β or anti-ETB antibody (5 µg) overnight at 4 °C with constant mixing. Protein A/G agarose beads (50 µl, 50% suspension) were then added and the samples were incubated for 3 h at 4 °C with constant mixing. After 3 washes with 50 mM Tris-HCl (pH 7.5) containing 150 mM NaCl, immune complexes were heated at 95 °C for 3 min in Laemmli sample buffer,

resolved on 12.5% SDS-PAGE gels, transferred to PVDF membranes, and analyzed for the presence of ETB or importin  $\beta$  immunoreactivity.

### 2.7. Immunoblot analysis

Following separation on SDS-PAGE, samples (50  $\mu$ g of protein) were electrophoretically transferred to PVDF membranes for 90 min at 100 V and 5 °C in transfer buffer containing 25 mM Tris base, 192 mM glycine and 5% methanol. Membranes were blocked by incubation for 2 h with 5% skim milk powder in 25 mM Tris-HCl pH 7.5, 150 mM NaCl and 0.05% Tween-20 (TBST), and then with the indicated primary antibody diluted 1:1000 in TBST containing 1% BSA for 16 h at 4 °C. The following day, membranes were washed with TBST (3 times, 10 min, room temperature) and then incubated for 2 h with the appropriate HRP-conjugated secondary antibody diluted 1:10,000 in blocking buffer. Following additional washing with TBST (3 times, 10 min), immune complexes were visualized by ECL and images acquired using Kodak BM-L or BM-R film.

### 2.9. Immunofluorescence

Freshly isolated adult ventricular myocytes were plated on laminin-coated coverslips for 1 h at 37 °C and then incubated with caged ET-1 (1  $\mu$ M) for 30 min at room temperature. Following incubation, cells were washed, placed on ice, and exposed to 3 min of UV light (black-ray long wave, model B100AP lamp, Thermo-Fisher) 3 cm above the plate to uncage the cET-1. Cells were then incubated at 37 °C for 15 and 30 min. Phosphorylation of CaMKII was evaluated by immunocytofluorescence as described previously with minor modifications [12, 13]. Briefly, cells were incubated for 90 min at room temperature with an anti-CaMKII phospho T286 antibody (Promega) diluted 1:50 in PBS containing 1% normal donkey serum.

## 2.10. Synthesis of a cell-permeable ETB antagonist

A caged analog of the ETB-selective antagonist, IRL2500, was prepared from the commercially available compound (Tocris Bioscience, Bristol, UK) following a method previously described for the synthesis of caged endothelin-1 [37]. Briefly, IRL2500 (10 mg; 1 equivalent; 17 mM) in 5 mL dichloromethane (DCM) was reacted with 4,5-dimethoxy-2-nitrobenzyl alcohol (19 mg; 5 equivalent, ~85 mM) in presence of 4-dimethylaminopyridine (0.7 mg; 0.3 equivalent, ~6 mM) and 1,3-dicyclohexylcarbodiimide (DCC) (18 mg; 5 equivalent, ~85 mM). The reaction, followed by analytical RP-HPLC, was completed within 4-5 h as observed by the disappearance of the starting material. Following the removal of the dicyclohexylurea formed during the esterification by filtration, the solvent was evaporated *in vacuo* and the resulting oil was extracted with H<sub>2</sub>O/DCM. Organic phases were combined, dried over MgSO<sub>4</sub>, filtered, and the solvent removed by evaporation. The crude caged IRL2500 was then dissolved in 0.25% of DMSO in water and purified by semi-preparative HPLC using a Vydac C18 column (10 μm, 250 x 10 mm) eluted with a linear gradient from eluent A to B (slope 1% B /2 min; eluent A = H<sub>2</sub>O, 0.1% trifluoroacetic acid, Eluent B = 100% acetonitrile, 0.1% trifluoroacetic acid). Fractions were collected and analyzed for caged IRL-2500 by analytical RP-HPLC using a Kromasil C18 column (5 μm, 100 Å, 250 x 4.6 mm) and MALDI-TOF mass spectrometry on an Applied Biosystems Voyager-DE spectrometer (Foster City, CA). Fractions containing the desired pure caged compound were pooled, dried, lyophilized and stored at -20 °C until further use. The addition of a 4,5-dimethoxynitrobenzyl (DMNB) group to IRL-2500 did not impede its ability to antagonize ligand binding to ETB (Supplemental Figure 1)

## 2.11. Ca<sup>2+</sup> imaging

Freshly isolated ventricular myocytes were plated on laminin-coated glass-bottomed culture dishes for 1 h at 37 °C in KB buffer. Cells were then incubated with Fluo-4 AM (5 μM)

in 10 mM HEPES (pH 7.4), 134 mM NaCl, 6 mM KCl, 10 mM glucose, 2 mM CaCl<sub>2</sub> and 1 mM MgCl<sub>2</sub> for 30 min at room temperature and in the absence or presence of a photolabile caged ET-1 analog ([Trp-ODMNB<sup>21</sup>]ET-1) [37] and the IP3R inhibitor 2-aminoethoxydiphenyl borate (2-APB), caged IRL-2500, BQ610, BQ-788, ryanodine, or vehicle, as indicated. Cells were then washed three times and incubated for 5 min with a cell-permeant fluorescent DNA dye, DRAQ5 (1 μM). Myocytes were then incubated an additional 15 min at room temperature to allow for de-esterification. Fluorescence imaging was accomplished using a Zeiss LSM 7 Duo microscope (combined LSM 710 and Zeiss Live systems) with a 63x/1.4 oil Plan-Apochromat objective. Fluo-4 was excited with a 488 nm/100 mW diode (1-5% laser intensity) and fluorescence emitted between 495 nm and 550 nm was collected. Cells were scanned at 30 fps in bi-directional mode. Pixel size was set at 0.2 μm and the pinhole at 2 Airy units. To visualize the nucleus, DRAQ5 was excited with a 635 nm/50 mW diode and fluorescence emitted at >655 nm was collected. Fluo-4 and DRAQ5 were excited and fluorescence collected simultaneously using 2 different Zeiss Live detectors. Images were acquired over a total period of 80 seconds (2000 frames). After acquiring 200 frames (6.7 s) to establish a baseline, caged ET-1 was photolysed by administering a 7 s pulse of UV light using a 405 nm/30 mW diode (100% laser intensity). DRAQ5 emissions were used to focus the UV laser into a 60 μm<sup>2</sup> rectangular region overlapping the nucleus. The microscope stage (Zeiss Observer Z1) was equipped with a BC 405/561 dichroic mirror that allowed simultaneous photolysis of the caged ET-1 (LSM 710 405 nm laser) and image acquisition (Zeiss Live). As the caged ligands used herein are photolysed upon exposure to UV, ratiometric Ca<sup>2+</sup> dyes could not be employed.

### 2.12. Statistical analysis

Data are presented as the mean ± the standard error of the mean (S.E.M.). The significance of differences between groups was determined using one-way ANOVA followed by Newman-Keul's Multiple Comparison tests (Prism 5.0d for Mac, GraphPad Software). Differences were considered significant when  $p < 0.05$ .

### 3. Results

#### 3.1. *Binding of fluorescent ET-1 and ET-3 analogs in isolated Triton X-100-skinned cardiomyocytes and nuclei isolated from cardiomyocytes*

Endothelin receptors have been previously demonstrated at the nuclear membrane in adult ventricular myocytes, [13, 17] and human vascular smooth muscle cells [15]. However, in our previous studies we observed faint ETA immunoreactivity in the perinuclear region of ventricular myocytes [12]. ETA binds ET-3 with 100-fold lower affinity than ET-1, whereas ETB binds ET-1 and ET-3 with equal affinity. Hence, to identify the endothelin receptor subtypes present on cardiac nuclear membranes we examined the binding of fluorescently-labeled ET-1 and ET-3 analogs to nuclear membranes in Triton-skinned rat ventricular myocytes and nuclei isolated from rat ventricular myocytes (Figure 1A). Nuclei were also stained with fluorescent DNA dye, DRAQ5. In isolated, skinned ventricular myocytes, rhodamine-ET-3 binding revealed a staining at the nuclear membrane and in the nucleoplasm as well as a striated pattern into the cytosol, suggesting the presence of ETRs on the transverse tubules (Figure 1A, Panels *a, b, e, f, i, j*). An enlargement of the nuclear region is shown in Panels *b, f, and j*. In nuclei isolated from rat ventricular myocytes, fluorescent labeling was observed at the nuclear membrane as well as the nucleoplasm (Figure 1A, Panels *c, d, g, h, k, i*). Three-dimensional rendering of deconvolved z-stacks revealed an intense staining at the nuclear membrane (Figure 1A, Panels *d, h, i*). Both rhodamine-ET-3 binding and rhodamine-ET-1 (7.5 nM) binding was displaced from nuclear membranes by the ETB-selective antagonist, BQ788 (1  $\mu$ M) (Figure 1B). Furthermore, the binding of rhodamine-ET-3 to nuclear membranes was also antagonized by BQ788 in Triton-skinned cardiomyocytes (Figure 1C). These results demonstrate that, although ETA predominates at the surface of ventricular myocytes [38, 39], the endothelin receptor subtype located at the nuclear membrane is ETB.

### 3.2 *Trafficking of ETB in ventricular myocytes*

We next sought to determine the source of ligand for ETB located on the nuclear envelope. An intracrine ligand may be synthesized endogenously or taken up by the target cell. In heterologous expression systems, ETB is constitutively internalized and traffics to the lysosomes for degradation [4, 40]; hence, one possibility is that in ventricular myocytes ETB and/or ETB-ligand complexes internalize and then translocate to the nuclear envelope. To test this hypothesis, we analyzed the internalization and trafficking of endothelin receptors in ventricular myocytes. Since the half-life of the ET:ETR complex is greater than 20 h [38, 41], we followed the internalization of ET:ETR complexes using fluorescent endothelin analogs in conjunction with confocal fluorescence microscopy. Figure 2 shows FAM-ET-1 fluorescence (left, green), LysoTracker (middle, red), or an overlay of both signals (right). FAM-ET-1 was rapidly internalized and demonstrated a highly punctate staining pattern characteristic of vesicular compartmentalization. The overlay indicates partial colocalization of FAM-ET-1 with LysoTracker (yellow).

Ventricular myocytes express ETA and ETB. As ET-1 is a ligand for both receptor subtypes, the images shown in Figure 2 represent the distribution of both ETA and ETB. At nanomolar concentrations, ET-3 binds ETB but not ETA. Thus, rhodamine-ET-3 was employed to selectively follow the trafficking of ET-3:ETB complexes. Figure 3 shows images of rhodamine-ET-3 fluorescence (left, red), LysoTracker (middle, green), or an overlay of both signals (right). Within 100 seconds of addition, ET-3 fluorescence was detected in vesicles stained with LysoTracker. Endocytosed ET-3:ETB complexes were never observed at nuclear or perinuclear membranes.

### 3.3 *Trafficking of ETB in endothelial cells*

ETA and ETB and are co-expressed in a variety of cells, including ventricular myocytes [38], and can form heterodimers that may differ from receptor monomers, and possibly

homodimers, with respect to endocytosis or trafficking itineraries [42, 43]. As aortic endothelial cells express only ETB, rat aortic endothelial cells were used to determine if the absence of ETA altered the trafficking of ET:ETB complexes (Figure 4). Within 400 seconds of rhodamine-ET-1 addition, all of the ET-1 fluorescence (left, red) was observed within the cells. A total colocalization of ET-1 and LysoTracker fluorescence was observed in the overlay (right, yellow). No rhodamine-ET-1 fluorescence was observed in the nuclear or perinuclear region.

### 3.4 Does ETB interact with importin $\beta$ 1

ETB contains a sequence of basic amino acids (KRFK) in the eighth helix that could serve as a classical nuclear localization sequence [44, 45]. Most proteins containing this type of sequence are transported from the cytoplasm into the nucleus by the importin  $\alpha/\beta$  heterodimer [46]. Once translocated, the nuclear localization sequence-importin complex dissociates and the importin returns to the cytoplasm. To determine if importin  $\beta$ 1 mediates the nuclear targeting of ETB, we investigated the possible presence of ETB:importin  $\beta$ 1 complexes by co-immunoprecipitation and immunoblot analyses (Figure 5 A,B). Antibody specificity and importin  $\beta$ 1 and ETB expression were confirmed by immunoblotting using whole cell lysates from porcine aortic endothelial cells, control HEK293 cells, a stable HEK293 cell line expressing ETB-V5 (V5 is a 14 amino acid epitope tag), and rat heart nuclei. Bands of 97-kDa (Figure 5A, left panel) and 50-kDa (Figure 5A, right panel), corresponding to the expected size of importin  $\beta$ 1 and ETB, respectively, were revealed. The interaction between ETB and importin  $\beta$ 1 was then studied by co-immunoprecipitation from porcine aortic endothelial cells, HEK 293 cells, and rat heart nuclei. Proteins were immunoprecipitated with an anti-ETB antibody and the resulting immune complexes were probed using an anti-importin  $\beta$ 1 antibody. No importin  $\beta$ 1 immunoreactivity was detected in ETB immunoprecipitates (Figure 5B, right panel). The reciprocal experiment yielded the same result (Figure 5B, left panel). Hence, ETB does not form a stable complex with importin  $\beta$ 1.

In order to confirm the immunoblotting results, we next studied the localization of ETB and importin  $\beta$ 1 in rat aortic endothelial cells (Figure 5C). Cells were fixed and decorated with antibodies directed against ETB (Figure 5C, Panels *a,b,c*; green) and importin  $\beta$ 1 (Figure 5C, Panels *d,e,f*; red). Cells were also labeled with a double-stranded DNA stain, TO-PRO-3, to delineate the nuclei (Figure 5C, Panels *j,k*; blue). As reported previously, ETB immunoreactivity was observed at the plasma membrane, intracellular compartments, and the nucleus [13]. Importin  $\beta$ 1 was located in the cytoplasm and at the nuclear envelope. To reduce the possibility of a false conclusion of colocalization, images were deconvolved using experimentally-derived point-spread functions, as described previously [13] (Figure 5C, Panels *c,f,i*). No voxels were identified as containing both ETB and importin  $\beta$ 1 immunoreactivity, indicating that these two proteins did not colocalize (Figure 5C, Panels *g,h,i*). The endocytosis of rhodamine-conjugated ET-3 was blocked when clathrin-mediated uptake was inhibited using dansylcadaverine (data not shown).

### 3.5. *ETB glycosylation*

N-glycosylation is a post-translational modification wherein high-mannose oligopolysaccharides are added to newly translated proteins in the ER and then modified to the final mature complex oligosaccharides in the Golgi apparatus as part of protein maturation and trafficking to the cell surface. ETB contains two potential sites for N-linked glycosylation [3] and has been shown to be glycosylated [47, 48]. Hence, to further determine if ETB translocates to the nucleus following endocytosis, we assessed the glycosylation status of ETB in nuclear membranes. Isolated nuclei were incubated in the presence or absence of peptide N-glycosidase F (PNGase F), an amidase that cleaves between the GlcNAc and asparagine residues of N-linked glycoproteins, thus removing both high mannose and complex glycosylations. No change in the electrophoretic mobility of ETB was observed (Supplemental Figure 2), suggesting that ETB located at nuclear membrane is not glycosylated. Whole-cell lysates from a stable HEK293 cell line constitutively expressing an ETB-V5 construct were used as a positive

control. Incubation with PNGase F induced a 2-kDa reduction in apparent molecular mass, indicating deglycosylation of ETB-V5. Hence, ETB on the nuclear envelope has not been modified by N-linked glycosylation, further suggesting that they are not derived from the cell surface.

An alternative source of ligand for endogenous ETB would be endogenous ET-1. All three ETs are synthesized as precursor proteins, preproETs, which are subsequently cleaved to pro-forms by furin-like proteases. The final step in ET biosynthesis involves the conversion of these pro-forms, Big-ETs by endothelin converting enzymes (ECEs). Processing by ECEs has been proposed to be a rate-limiting step in endothelin biosynthesis. Ventricular myocytes express ET-1 and the intracellular levels of ET-1 mRNA are reduced by extracellular ET-1 (Supplemental Figure 3). Although these cells express both ETA and ETB at the cell surface [38, 39], the ETA antagonist BQ610 prevented the ET-1-promoted reduction in ET-1 mRNA whereas an ETB antagonist BQ788 did not. Together these data suggest that ET-1 is generated intracellularly and, that extracellular ET-1 may actually suppress intracrine ET-1 signalling.

### *3.6. Signalling by intracellular ET-1*

Extracellular ET-1 induces an IP<sub>3</sub>-dependent release of Ca<sup>2+</sup> from the nuclear cisternae in ventricular myocytes [49]. Hence, we examined the ability of nuclear ETB activation to alter nuclear Ca<sup>2+</sup> levels. ET-1 induces Ca<sup>2+</sup> release from nuclei isolated from rat heart [12]: however, these preparations include nuclei from multiple cell types. To determine if intracellular ET-1 induces the release of Ca<sup>2+</sup> into the nucleoplasm within the context of an intact ventricular myocyte, a photolabile caged ET-1 analog ([Trp-ODMNB<sup>21</sup>]ET-1) [37] was employed and changes in [Ca<sup>2+</sup>] were determined using the cell permeant fluorescent Ca<sup>2+</sup> dye, Fluo-4 AM. DRAQ5 fluorescence was used to determine the position of the nucleus and changes in nucleoplasmic Fluo-4 fluorescence were quantified. Three different concentrations of caged ET-1 (cET-1) were tested (10<sup>-5</sup>, 10<sup>-6</sup>, and 10<sup>-7</sup> M) in the loading buffer. cET-1 release (405 nm/30 mW diode. 100% laser intensity, 7 s) caused a concentration-dependent increase in

nucleoplasmic  $[Ca^{2+}]_n$  ( $[Ca^{2+}]_n$ ), which was significant at cET-1 concentrations of  $10^{-6}$  and  $10^{-5}$  M (Figure 6A) in the loading buffer. Note that UV irradiation induced a transient increase in Fluo-4 fluorescence in all conditions including the irradiated control (no cET-1). No increase in  $[Ca^{2+}]_n$  was observed in myocytes where cET-1 was excluded from the loading buffer. Addition of ETA- (BQ610) and ETB-selective (BQ788) antagonists ( $1 \mu\text{M}$ ) to the extracellular medium failed to block the ability of cET-1 to increase  $[Ca^{2+}]_n$  (Figure 6B). Thus, photolysed ET-1 was not leaving the cells and activating ETRs at the cell surface but, instead, acting directly on intracellular ETB. As an additional control, we developed a caged, cell-permeable analog of the ETB-selective antagonist IRL-2500. The addition of a 4,5-dimethoxynitrobenzyl (DMNB) group to IRL-2500 did not impede its ability to antagonize ligand binding to ETB (Supplemental Figure 1, Figure 7A). Loading ventricular myocytes with cIRL-2500 in addition to cET-1 prevented cET-1 from increasing  $[Ca^{2+}]_n$  (Figure 7B). The increase in  $[Ca^{2+}]_n$  following photolysis of caged ET-1 was attenuated, but was not completely blocked, by an inhibitor of the inositol trisphosphate receptor (IP3R), 2-aminoethoxydiphenyl borate (2-APB,  $20 \mu\text{M}$ ) (Figure 8). Concentrations of 2-APB as high as  $100 \mu\text{M}$  failed to produce a complete block of the increase in  $[Ca^{2+}]_n$  evoked upon photolysis of cET-1 (data not shown). Although cytosolic  $[Ca^{2+}]$  also increased (Figure 8A), a direct comparison of changes in cytosolic and nuclear  $[Ca^{2+}]$  could not be made due to differences in calcium buffering and the properties of Fluo-4 in these compartments [50, 51]. The sarcoplasmic reticulum and perinuclear space are interconnected such that  $Ca^{2+}$  is free to exchange between these compartments [52]. As ryanodine depletes the SR calcium stores [53], we examined the effect of uncaging cET-1 on  $[Ca^{2+}]_n$  following preincubation with ryanodine. In the presence of ryanodine, intracellular release of ET-1 failed to increase  $[Ca^{2+}]_n$ , confirming that activation of nuclear ETB resulted in release of  $Ca^{2+}$  from SR-perinuclear stores (Figure 8B,C). Thus, intracellular release of ET-1 activated nuclear ETB, inducing a ryanodine-sensitive increase in  $[Ca^{2+}]_n$  that involved both 2-APB-sensitive and 2-APB-insensitive  $Ca^{2+}$  channels: the 2-APB-sensitive component is likely due to activation of IP3R.

Extracellular ET-1 induces an increase in  $[Ca^{2+}]_n$  in rabbit ventricular myocytes via activation of IP3R on the nuclear membranes, which, in turn, leads to an increase in active  $Ca^{2+}$ /calmodulin-dependent protein kinase II (CaMKII) within the nucleus [49, 54]. Thus, we next sought to determine if elevation of intracellular [ET-1] affected CaMKII activity in the nucleus. The ability of cET-1 to induce changes in CaMKII autophosphorylation was evaluated in ventricular myocytes by immunocytochemistry. At 15 and 30 min following release of ET-1 by photolysis cET-1, cells were fixed and then decorated with antibodies directed against phospho-CaMKII threonine-286. Nuclei were stained with TO-PRO3. To evaluate autophosphorylation of CaMKII, fluorescence intensity was measured in maximum intensity projections. A significant increase in phosphorylation of CaMKII was observed within the nucleus following photolysis of caged ET-1 (Figure 9).

#### 4. Discussion

Plasma membrane GPCRs are known to regulate a wide variety of biological responses. Recently, however, functional GPCRs have also been demonstrated on intracellular membranes including the mitochondria [55] and nuclear envelope (reviewed in [11, 14]). The functions of endogenous GPCRs remain to be established.

Nuclear localization of endothelin receptors has been demonstrated in rat liver [56], rat cardiomyocytes [12], and mouse spiral ganglion neurons [57]. We previously reported that ETB immunoreactivity was primarily associated with nuclear membranes in ventricular myocytes whereas ETA was associated with the cell surface and T-tubular network as well as showing a weaker association with nuclear or perinuclear membranes [12, 13]. Using fluorescently-labeled ET-1 and ET-3 analogs we observed binding patterns similar to those we observed previously by immunocytochemistry; however, BQ788, a selective antagonist of ETB, attenuated the binding of both rhodamine-ET-3 and rhodamine-ET-1 to nuclear membranes, thus confirming that the endothelin receptor subtype on nuclear membranes in ventricular myocytes is ETB. We also demonstrate that nuclear ETB does not bind importin  $\beta$ 1, have not transited the ER-Golgi network to the cell surface, and do not translocate from the cell surface to nuclear membranes following endocytosis. Furthermore, the intracellular release of a photolabile, caged ET-1 analog induced an IP3-mediated increase in  $[Ca^{2+}]_n$  in intact ventricular myocytes. This increase was prevented by loading ventricular myocytes with a cell-permeable ETB-selective antagonist, but not by extracellular ETA and ETB antagonists, indicating the ability of nuclear ETB to regulate  $Ca^{2+}$  signalling within the nucleus.

In heterologous expression systems, ETA localize primarily to the plasma membrane [4], internalize in a ligand-dependent manner [58], and then follow a recycling pathway through the pericentriolar recycling compartment and then back to the plasma membrane [5]. In contrast, ETB internalizes constitutively, without a requirement for ligand binding, and then translocates to the lysosomes for degradation [5, 40]. The fate of each receptor subtype is under the control of specific elements regulating protein trafficking. Chimeric ETA and ETB constructs reveal the cytoplasmic C-terminal domain of ETA is sufficient to specify receptor recycling whereas the comparable domain in ETB specifies delivery to lysosomes [4, 6]. In ventricular myocytes

[12] and mouse spiral ganglion neurons [57], which express both ETA and ETB, ETB is primarily associated with the nuclear membranes whereas ETA is at the cell surface. Hence, it is unlikely that the presence of ETB on nuclear membranes is a result of 'overflow' from the endoplasmic reticulum. Interestingly, both ETA and ETB, along with several other GPCRs, possess a nuclear localization sequence within their carboxyl tail region [44, 59]. The presence of a similar nuclear localization sequence in both ETA and ETB implies the presence of additional structural determinants that either direct ETB to segregate to the nucleus or ETA to the plasma membrane. Both  $\alpha$ 1A- and  $\alpha$ 1B-adrenergic receptors are found on nuclear membranes in ventricular myocytes [59, 60] and both were recently shown to possess nuclear localization sequence motifs within their C-terminal domains, although, interestingly, not the same type of nuclear localization sequence [59]. In either case, site-directed mutations within this sequence prevented sorting of either receptor to the nucleus, but did not result in their relocalization to the plasma membrane [59]. Furthermore, when stably expressed in HEK293 cells, ETB localizes primarily to the plasma membrane [61] (Merlen and Allen, unpublished). Hence there may also be cell-specific factors involved in directing the localization of GPCRs, including ETB, to the nuclear membranes.

Intracrine signalling refers to a process whereby a ligand, originating within a target cell or taken up from the extracellular milieu, acts upon an intracellular receptor (reviewed in [9-11, 62-67]). The origin of the ligand for endogenous endothelin receptors remains unknown. Molecules with a suitable partition coefficient may diffuse across the plasma membrane whereas small charged molecules could pass through channels or be taken up by transporters. Catecholamines, for example, can cross both the plasma membrane and nuclear membranes, thus accessing the ligand binding site within the nuclear cisternae, in ventricular myocytes via the extraneuronal monoamine transporter (EMT/OCT3) [60]. One possible source for intracellular endothelin would be endocytosis: once formed at the cell surface, receptor-ligand complexes translocate to the nuclear membranes. In the present study we investigated the trafficking of ET:ETR complexes in ventricular myocytes, rat aortic endothelial cells and

porcine aortic endothelial cells using fluorescently-labeled ET-1 and ET-3 in order to determine if: 1) ETB on the nuclear membranes is a result of post-endocytotic trafficking and 2) extracellular endothelin has access to ETB on nuclear membranes. At no time was extracellularly applied rhodamine-endothelin fluorescence detected at the nuclear membrane. An alternative possibility to endogenous endothelin receptors being regulated by exogenous endothelins is that endothelin produced within the target cell acts as an intracrine ligand for endogenous receptors. Processing by ECEs has been proposed to be a rate-limiting step in endothelin biosynthesis. ECE-1 has been found in cytosol and nuclei in ventricular myocytes and in nuclei isolated from rat heart. There are 4 known splice variants of ECE-1 (ECE-1 a-d). ECE-1a and ECE-1c are expressed in ventricular myocytes [68] and ECE-1c expression is upregulated 5-fold in cardiomyocytes following congestive heart failure [68]. Nuclear localization of ECE-1a and ECE-1b has already been demonstrated in human microvascular endothelial cells, human umbilical vein endothelial cells, and transfected CHO cells [69, 70]. Moreover, ET-1 is produced, stored and secreted by neonatal [71] and adult cardiac ventricular myocytes [72] under basal conditions, and regulated in response to stretch [73], electrical stimulation [72], or extracellular ET-1 (Supplemental Figure 2). Interestingly, although the basal level of ET-1 production in ventricular myocytes from failing hearts is unchanged, the effect of electrical stimulation on ET-1 secretion is reduced [72]. In endothelial cells, ET-1 production is regulated at the level of transcription, mRNA stability, and maturation of the ET precursor protein, preproendothelin. Whereas extracellular ET-1 reduces the cellular content of ET-1 mRNA in endothelial cells [74], Ang II, oxidized LDL, insulin, isoproterenol, thrombin, TGF $\beta$ , TNF $\alpha$ , verotoxin, and VEGF increase ET-1 mRNA abundance [75-77]. The best characterized intracrine signalling system is that of peptidergic agonist, Ang II. AT1R and AT2R have been demonstrated on the nuclear membranes in cardiomyocytes [11], hepatocytes, and vascular smooth muscle cell lines [78, 79]. Ventricular myocytes express angiotensin and angiotensin converting enzyme (ACE) immunoreactivity is detected in nuclei of cultured rat cardiomyocytes and fibroblasts as well as mesangial cells cultured from spontaneously

hypertensive rats [80, 81]. Thus, Ang II can be generated intracellularly. There is also evidence that intracellular Ang II (iAng II) levels change in various forms of cardiomyopathy [82]. Transduction of neonatal rat ventricular myocytes with an adenoviral construct expressing Ang II led to the rapid induction of cellular hypertrophy [83]. Furthermore, transgenic mice engineered for cardiomyocyte-specific overexpression of rat angiotensinogen, as driven by the mouse  $\alpha$ -myosin heavy chain (MHC) promoter, show increased levels of iAng II and also develop cardiac hypertrophy [84]. Hence, intracrine signalling may be involved in pathologic cardiac remodelling.

Extracellular ET-1 acts on cell surface ETRs to increase IP3 production in ventricular myocytes [85]. Increasing IP3 production, in turn, increases  $[Ca^{2+}]_n$  through an IP3R-mediated release of  $Ca^{2+}$  from perinuclear stores in both atrial and ventricular myocytes [49, 86, 87]. ET-1 has also been shown to increase  $[Ca^{2+}]_n$ , presumably released from stores within the nuclear cisternae, in nuclei isolated from chick heart, cultured human aortic smooth muscle cells [15, 88] and rat heart [12]. Similarly, the ETB-selective agonist IRL-1620 increases  $[Ca^{2+}]_n$  in nuclei isolated from rat heart [12] and liver [89]. This release of  $Ca^{2+}$  represents activation of calcium channels within the inner nuclear membranes (see [90]); however, the actual mechanism whereby  $[Ca^{2+}]_n$  was increased was not assessed. We have now shown that treatment of intact ventricular myocytes with a caged ET-1 analog also induced an IP3R-mediated increase in  $[Ca^{2+}]_n$ . This increase was prevented by a cell-permeable analog of an ETB-selective antagonist, IRL-2500, but not by adding BQ610 and BQ788 to the extracellular medium, thus confirming a direct role of nuclear ETB in regulating nuclear  $Ca^{2+}$  signalling in intact ventricular myocytes. Other GPCRs found in nuclear membranes have also been shown to increase  $[Ca^{2+}]_n$  including Ang II [18, 91], bradykinin B2 [21], prostaglandin  $E_2$  [22-24], lysophosphatidic acid type-1 [25, 26], and metabotropic glutamate type-5 [92-95].

IP3R-mediated  $Ca^{2+}$ -release is involved in hypertrophy induced by isoproterenol and Ang II but not by constriction of the transverse aorta [96]. The increase in  $[Ca^{2+}]_n$  mediated by IP3R activates CaMKII $\delta$  within the nucleus. When activated, CaMKII $\delta$  phosphorylates histone

deacetylase 5 (HDAC5) at serine-259 and serine-498, resulting in its binding a 14-3-3 chaperone and translocation to the cytoplasm [49]. Within the nucleus, HDAC5 binds to and suppresses the transcriptional activity of myocyte enhancing factor-2 (MEF2), thus preventing transcription of genes involved in hypertrophy (e.g.,  $\beta$ -myosin heavy chain, atrial natriuretic peptide, brain natriuretic peptide). We have shown that photolysis of intracellular cET-1 induced both an IP3R-mediated increase in  $[Ca^{2+}]_n$  and an increase in activated CaMKII within the nucleus. Hence, like ETRs at the cell surface, activation of ETB on the nuclear envelope may result in expression of MEF2-dependent genes.

The use of a caged-ET1 analog has allowed us to specifically target intracellular ETB and study its function. Similarly, cell permeable and cell impermeable antagonists were recently used to demonstrate that muscarinic and  $\alpha_1$ -adrenergic receptors play distinct roles in function of their localization [97, 98]. Considering the number of GPCRs, and their effectors, now known to localize to the nuclear membrane, the biological response evoked upon activation of a given GPCR may be a result of the integration of signalling pathways activated at the plasma membrane and the nuclear membrane.

A potential limitation of the present study is the lack of specific IP3R inhibitors. Intracellular release of ET-1 by photolysis of cET-1 resulted in an increase in  $[Ca^{2+}]_n$  that was partially blocked by the IP3R inhibitor, 2-APB. However, IP3R inhibitors such as 2-APB and the xestospongins have multiple cellular targets, including IP3R, store-operated  $Ca^{2+}$  entry (SOC), and SERCA [99, 100]. In addition, the effect of 2-APB on SOC is dose-dependent: 30-50  $\mu$ M 2-APB is inhibitory whereas lower concentrations of 2-APB stimulate SOC [101]. However, with this said, the 2-APB-sensitive component of the increase in  $[Ca^{2+}]_n$  evoked by increasing the intracellular ET-1 concentration is likely mediated by IP3R: the identity of the 2-APB-insensitive channel remains to be determined.

## 5. Conclusions

We have shown that the endothelin receptor subtype present on cardiac nuclear membranes is ETB. ETB is constitutively present on the nuclear envelope rather than being translocated there from the cell surface upon ligand binding. Furthermore, these receptors are not accessible to extracellular ET, implicating endogenous ET-1 as the intracrine ligand for these receptors. Finally, nuclear ETB induces an IP3-dependent increase in  $[Ca^{2+}]_n$  in response to cytoplasmic release of ET-1 and this increase in  $[Ca^{2+}]_n$  was accompanied by an increase in activate CaMKII within the nucleus. Our results demonstrate that ETB on the nuclear envelope may play a distinct role in stimulus-transcription coupling.

## **Acknowledgements**

The authors are grateful to Ms. Bahira Hussein for technical assistance. This work was supported by grants from the Heart and Stroke Foundation of Quebec and the Canadian Institutes for Health Research (grant number MOP-64183, MOP-125970) to BGA. BGA was a New Investigator of the Heart and Stroke Foundation of Canada and a Senior Scholar of the Fondation de la Recherche en Santé du Québec (FRSQ). SN holds the Paul-David Chair in Cardiovascular Electrophysiology. CM is the recipient of a fellowship from the Heart and Stroke Foundation of Canada. NF received a research traineeship from the Heart and Stroke Foundation of Canada. AT is recipient of FRSQ-RSCV/HSFQ doctoral scholarship.

## Abbreviations

\*The abbreviations used are: 2-APB, 2-aminoethoxydiphenyl borate;; Ang II, Angiotensin II;  $\alpha$ AR,  $\alpha$ -adrenergic receptor;  $[Ca^{2+}]_n$ , nucleoplasmic free calcium concentration; CaMKII,  $Ca^{2+}$ /calmodulin-dependent protein kinase II; DMNB, 4,5-dimethoxynitrobenzyl group; DNA, deoxyribonucleic acid; DCC, 1,3-dicyclohexylcarbodiimide; DCM, dichloromethane; DTT, dithiothreitol; ECE1-a, endothelin converting enzyme 1a; cET-1, caged ET-1; caged ET-1, [Trp-ODMNB<sup>21</sup>]ET-1; ET-1, endothelin 1; ET-2, endothelin 2; ET-3, endothelin 3; ETA, endothelin type A receptor; ETB, endothelin type B receptor; ETR, endothelin receptor; GPCR, G protein-coupled receptor; HDAC5; histone deacetylase 5; IP3, inositol 1,4,5-trisphosphate; IP3R, inositol 1,4,5-trisphosphate receptor; ISO, isoproterenol; MEF2, myocyte enhancing factor-2; PBS, phosphate buffered saline; PMSF, phenylmethanesulphonylfluoride; PNGase F, peptide N-glycosidase F; qPCR, quantitative real-time polymerase chain reaction; RNA, ribonucleic acid; RyR, ryanodine receptor; TCA, trichloroacetic acid; TFA, trifluoroacetic acid; TX-100, Triton X-100.

## Figure legends

**Figure 1. Binding of rhodamine-ET-3 and rhodamine-ET-1 in Triton-skinned ventricular myocytes and nuclei isolated from ventricular myocytes. A).** Freshly isolated adult rat ventricular myocytes were permeabilized with Triton and then plated on laminin-coated Fluorodish culture dishes. Skinned cells were then incubated 30 min with 0.1  $\mu\text{M}$  rhodamine-ET-3 at room temperature. Cells were then washed and DRAQ5, a fluorescent DNA dye was added to stain nuclei. Panels b, f, and j (Scale Bar = 5  $\mu\text{m}$ ) show a single nucleus from Panels a, e, and i at higher magnification. Panels c, g and k show an isolated nucleus similarly stained with rhodamine ET-3 and DRAQ5. In panels d, h, and l (Scale Bar = 1  $\mu\text{m}$ ) the image stacks for the nuclei shown in the above panels have been deconvolved (Huygens Professional Imaging Software) and then rendered to create 3D images (Volocity 3D Image Analysis Software). **B).** Nuclei were prepared from freshly isolated adult rat cardiac myocytes, plated on laminin-coated Fluorodish culture dishes and then preincubated with 1  $\mu\text{M}$  ETB-selective antagonist BQ788 for 30 min at room temperature. Rhodamine ET-3 or rhodamine ET-1 (7.5 nM) was added for additional 30 min incubation. Nuclei were then washed 3 times and stained with fluorescent DNA dye, DRAQ5. Scale Bar = 4.8  $\mu\text{m}$ . **C).** Freshly isolated adult rat ventricular myocytes were permeabilized with Triton and then plated on laminin-coated Fluorodish culture dishes. Skinned cells were then preincubated with 1  $\mu\text{M}$  ETB-selective antagonist BQ788 for 30 min at room temperature. Rhodamine ET-3 (7.5 nM) was added for additional 30 min incubation. Cells were then washed three times and DRAQ5 was added to stain nuclei. Images were acquired using a Zeiss LSM 710 confocal microscope. Scale Bar = 2.3  $\mu\text{m}$ .

**Figure 2. Endocytosis and trafficking of FAM-ET-1 in ventricular myocytes.** Freshly isolated rat ventricular myocytes were plated on laminin-coated coverslips and then treated with 30 nM LysoTracker for 15 min at 37  $^{\circ}\text{C}$ , washed and then incubated with 10 nM FAM-ET-1 at room temperature. FAM-ET-1 fluorescence is shown in green and LysoTracker is shown in red. Merged images on the right indicate the extent of colocalization (yellow). Fluorescent images

were acquired every 10 s at two emission wavelengths (488 and 543 nm): images acquired at 100, 500, 900, and 1,300 s after the application of FAM-ET-1 are shown. Bottom panel shows the corresponding differential interference contrast image. The arrow indicates the position of the nucleus. Scale Bar = 10  $\mu$ m.

**Figure 3. Endocytosis and trafficking of rhodamine-ET-3 in ventricular myocytes.** Freshly isolated rat ventricular myocytes were plated on laminin-coated coverslips and then treated with 30 nM LysoTracker for 15 min at 37 °C, washed and then incubated with 5 nM rhodamine-ET-3 at room temperature. Rhodamine-ET-3 fluorescence is shown in red and LysoTracker is shown in green. Merged images on the right indicate the extent of colocalization (yellow). Bottom panel shows the corresponding differential interference contrast image. Fluorescent images were acquired every 10 s at two emission wavelengths (488 and 543 nm): images acquired at 100, 500, 900, and 1,300 s after the application of Rhodamine-ET-3 are shown. The arrow indicates the position of the nucleus. Scale Bar = 10  $\mu$ m.

**Figure 4. Endocytosis and trafficking of rhodamine-ET-1 in rat aortic endothelial cells.** Serum-starved rat aortic endothelial cells were preincubated with 10 nM LysoTracker green at 37 °C, washed, and then incubated with 10 nM rhodamine-ET-1 at room temperature. Rhodamine-ET-1 fluorescence is shown in red and LysoTracker is shown in green. Merged images on the right indicate the extent of colocalization (yellow). Fluorescent images were acquired every 10 s at two emission wavelengths (488 and 543 nm): images acquired at 0, 200, 400, and 600 s after the application of Rhodamine-ET-1 are shown. The bottom panel is a difference interference contrast image. The arrow indicates the position of the nucleus. Scale Bar = 10  $\mu$ m.

**Figure 5. ETB does not interact with importin  $\beta$ 1.** **A)** Expression of ETB and importin  $\beta$ 1 was confirmed in porcine aortic endothelial cells, HEK293 cells and nuclei isolated from rat heart by immunoblotting. **B)** Lysates from porcine aortic endothelial cells, HEK293 cells, and

isolated nuclei were incubated with anti-ETB or anti-importin  $\beta$ 1 antibodies, as indicated. Nuclei were pre-incubated in the presence (+) or absence (-) of ET-1 (0.1  $\mu$ M, 37 °C, 5 min). Nuclei\*, omission of antibody from the immunoprecipitation reaction. Arrowhead indicates bands corresponding to the heavy and light chains of the precipitating antibody. Numbers to the left indicate the positions of the prestained molecular mass markers proteins. C) Immunofluorescence staining of rat aortic endothelial cells for ETB and importin  $\beta$ 1. Cells were fixed and then incubated with anti-ETB (panels a,b,c) and anti-importin  $\beta$ 1 (panels d,e,f) antibodies. The cells were also stained with TO-PRO-3 to reveal nuclei (panels j,k). Images b, e, h, and k show an enlargement of the nucleus. Images were also deconvolved (panels c,f,i). Panel l shows the corresponding differential interference contrast image.

**Figure 6. Intracellular photolysis of a caged ET-1 analog induces an increase in nucleoplasmic  $[Ca^{2+}]_n$ .** A) Nucleoplasmic  $[Ca^{2+}]_n$  recorded in rat ventricular myocytes before and after photolysis in cells preincubated with caged ET-1 at 10  $\mu$ M, 1  $\mu$ M, 0.1  $\mu$ M or vehicle. B) Nucleoplasmic  $[Ca^{2+}]_n$  recorded before and after photolysis in cells preincubated with 1  $\mu$ M caged ET-1, caged ET-1 plus BQ610 (ETA antagonist) and BQ788 (ETB antagonist) (BQ; 1  $\mu$ M each) or media alone (control). Controls were performed both with (control + uv) and without (control - uv) UV irradiation. DRAQ5 fluorescence was used to select the region corresponding to the nucleoplasm. Signals are presented as background-subtracted normalized fluorescence ( $\%F/F_0$ ), where F is the fluorescence intensity, and  $F_0$  is the resting fluorescence recorded in the same cell under steady-state conditions prior to photolysis. For each condition, the mean  $\pm$  s.e.m. of nucleoplasmic Fluo-4 fluorescence at 30 s or 50 s (as indicated) after photolysis is presented as a histogram. Number of cells is indicated in parentheses. \*,  $p < 0.05$ ; \*\*,  $p < 0.01$ ; \*\*\*,  $p < 0.001$ .

**Figure 7. A caged IRL2500 analog inhibits rhodamine-ET-3 binding in isolated nuclei and the increase in  $[Ca^{2+}]_n$  induced by caged ET-1.** A) Nuclei freshly isolated from rat ventricular myocytes were plated onto a laminin-coated Fluorodish and preincubated for 30 min with

photolysed (uIRL2500) or not photolysed (cIRL2500) caged IRL2500 ( $10^{-6}$  M). Rhodamine ET-3 ( $7.5 \times 10^{-9}$  M) was then added for an additional 30 min incubation. Following three washes, nuclei were stained with fluorescent DNA dye, DRAQ5. Images were acquired using a Zeiss LSM 710 microscope. Scale Bar = 4.8  $\mu$ m. **B**) Changes in nucleoplasmic  $[Ca^{2+}]$  were recorded, as described in Materials and Methods, before and after photolysis in cells preincubated with or without caged ET-1 (cET-1) and in presence or absence of caged IRL2500 (cIRL2500). DRAQ5 was used to target a region corresponding to the nucleoplasm. Signals are presented as background-subtracted normalized fluorescence ( $\%F/F_0$ ), where F is the fluorescence intensity, and  $F_0$  is the resting fluorescence recorded in the same cell under steady-state conditions prior to photolysis. For each condition, the mean  $\pm$  s.e.m. of nucleoplasmic Fluo-4 fluorescence at 50 s is presented.

**Figure 8. Ryanodine and 2-APB inhibit the increase in nucleoplasmic  $[Ca^{2+}]$  induced by photolysis of a caged ET-1.** **A**) Nucleoplasmic  $[Ca^{2+}]$  recorded in rat ventricular myocytes before and after photolysis in cells preincubated with vehicle, 1  $\mu$ M caged ET-1 (cET-1), or 1  $\mu$ M caged ET-1 plus 20  $\mu$ M 2-APB. **B**) Nucleoplasmic  $[Ca^{2+}]$  recorded before and after photolysis in cells preincubated with 1  $\mu$ M caged ET-1 (cET-1), caged ET-1 plus 20  $\mu$ M 2-APB, ryanodine (Rya) or media alone (control). Controls were performed both with (control + uv) and without (control - uv) uv irradiation. DRAQ5 fluorescence was used to select the region corresponding to the nucleoplasm. Signals are presented as background-subtracted normalized fluorescence ( $\%F/F_0$ ), where F is the fluorescence intensity, and  $F_0$  is the resting fluorescence recorded in the same cell under steady-state conditions prior to photolysis. **C**) For each condition shown in Panel B, the mean  $\pm$  s.e.m. of nucleoplasmic Fluo-4 fluorescence at 30 s after photolysis is presented as a histogram. Number of cells is indicated in parentheses. \*,  $p < 0.05$ ; \*\*,  $p < 0.01$ ; \*\*\*,  $p < 0.001$ .

**Figure 9. Intracellular photolysis of a caged ET-1 analog induces activation of CaMKII within the nucleus.** Autophosphorylation of CaMKII was studied by immunofluorescence in

rat ventricular myocytes treated with cET-1 (1  $\mu$ M) or vehicle. Ventricular myocytes were incubated with cET-1 for 30 min at room temperature. Following incubation, cells were washed, placed on ice, and exposed to a UV lamp for 3 min. Cells were then incubated at 37 °C for 15 (upper panels) or 30 (lower panels) min, fixed, and labeled with an antibody directed against phospho-CaMKII threonine-286 (red). Nuclei were stained with TO-PRO-3 (blue). Maximum intensity projection was performed to measure fluorescence intensity associated with phospho-CaMKII. Fluorescence intensity was determined in nuclei (Fnuc) and cytoplasm (Fcyto) and normalized to total area of the nucleus or cell. \*\*, p<0.01.

**Disclosure:**

The authors declare no conflicts of interest.

## References

- [1] Sokolovsky M. Endothelin receptor heterogeneity, G-proteins, and signaling via cAMP and cGMP cascades. *Cell Mol Neurobiol.* 1995;15:561-71.
- [2] Arai H, Hori S, Aramori I, Ohkubo H, Nakanishi S. Cloning and expression of a cDNA encoding an endothelin receptor. *Nature.* 1990;348:730-2.
- [3] Sakurai T, Yanagisawa M, Takawa Y, Miyazaki H, Kimura S, Goto K, et al. Cloning of a cDNA encoding a non-isopeptide-selective subtype of the endothelin receptor. *Nature.* 1990;348:732-5.
- [4] Abe Y, Nakayama K, Yamanaka A, Sakurai T, Goto K. Subtype-specific trafficking of endothelin receptors. *J Biol Chem.* 2000;275:8664-71.
- [5] Bremnes T, Paasche JD, Mehlum A, Sandberg C, Bremnes B, Attramadal H. Regulation and intracellular trafficking pathways of the endothelin receptors. *J Biol Chem.* 2000;275:17596-604.
- [6] Paasche JD, Attramadal T, Sandberg C, Johansen HK, Attramadal H. Mechanisms of endothelin receptor subtype-specific targeting to distinct intracellular trafficking pathways. *J Biol Chem.* 2001;276:34041-50.
- [7] Tamamori M, Ito H, Adachi S, Akimoto H, Marumo F, Hiroe M. Endothelin-3 induces hypertrophy of cardiomyocytes by the endogenous endothelin-1-mediated mechanism. *J Clin Invest.* 1996;97:366-72.
- [8] Yang LL, Gros R, Kabir MG, Sadi A, Gotlieb AI, Husain M, et al. Conditional cardiac overexpression of endothelin-1 induces inflammation and dilated cardiomyopathy in mice. *Circulation.* 2004;109:255-61.

- [9] Bkaily G, Avedanian L, Al-Khoury J, Provost C, Nader M, D'Orleans-Juste P, et al. Nuclear membrane receptors for ET-1 in cardiovascular function. *Am J Physiol Regul Integr Comp Physiol.* 2011;300:R251-R63.
- [10] Vaniotis G, Allen BG, Hébert TE. Nuclear GPCRs in cardiomyocytes: an insider's view of  $\beta$ -adrenergic receptor signaling. *Am J Physiol Heart Circ Physiol.* 2011;301:H1754-H64.
- [11] Tadevosyan A, Vaniotis G, Allen BG, Hebert TE, Nattel S. G protein-coupled receptor signalling in the cardiac nuclear membrane: evidence and possible roles in physiological and pathophysiological function. *J Physiol.* 2012;590:1313-30.
- [12] Boivin B, Chevalier D, Villeneuve LR, Rousseau E, Allen BG. Functional endothelin receptors are present on nuclei in cardiac ventricular myocytes. *J Biol Chem.* 2003;278:29153-63.
- [13] Boivin B, Villeneuve LR, Farhat N, Chevalier D, Allen BG. Subcellular distribution of endothelin signalling pathway components in ventricular myocytes and heart: Lack of preformed caveolar signalosomes. *J Mol Cell Cardiol.* 2005;38:665-76.
- [14] Boivin B, Vaniotis G, Allen BG, Hébert TE. G protein-coupled receptors in and on the cell nucleus: a new signalling paradigm? *J Recept Signal Transduct Res.* 2008;28:15-28.
- [15] Bkaily G, Choufani S, Hassan G, El-Bizri N, Jacques D, D'Orleans-Juste P. Presence of functional endothelin-1 receptors in nuclear membranes of human aortic vascular smooth muscle cells. *J Cardiovasc Pharmacol.* 2000;36:S414-S7.
- [16] Vaniotis G, Del Duca D, Trieu P, Rohlicek CV, Hebert TE, Allen BG. Nuclear  $\beta$ -adrenergic receptors modulate gene expression in adult rat heart. *Cell Signal.* 2011;23:89-98.

- [17] Boivin B, Lavoie C, Vaniotis G, Baragli A, Villeneuve LR, Ethier N, et al. Functional  $\beta$ -adrenergic receptor signalling on nuclear membranes in adult rat and mouse ventricular cardiomyocytes. *Cardiovasc Res.* 2006;71:69-78.
- [18] Tadevosyan A, Maguy A, Villeneuve LR, Babin J, Bonnefoy A, Allen BG, et al. Nuclear-delimited angiotensin receptor-mediated signaling regulates cardiomyocyte gene expression. *J Biol Chem.* 2010;295:22338-49.
- [19] Ventura C, Maioli M, Pintus G, Posadino AM, Tadolini B. Nuclear opioid receptors activate opioid peptide gene transcription in isolated myocardial nuclei. *J Biol Chem.* 1998;273:13383-6.
- [20] Eggena P, Zhu JH, Clegg K, Barrett JD. Nuclear angiotensin receptors induce transcription of renin and angiotensinogen mRNA. *Hypertension.* 1993;22:496-501.
- [21] Savard M, Barbaz D, Belanger S, Muller-Esterl W, Bkaily G, D'Orleans-Juste P, et al. Expression of endogenous nuclear bradykinin B2 receptors mediating signaling in immediate early gene activation. *J Cell Physiol.* 2008;216:234-44.
- [22] Bhattacharya M, Peri KG, Almazan G, Ribeiro-da-Silva A, Shichi H, Durocher Y, et al. Nuclear localization of prostaglandin E2 receptors. *Proc Natl Acad Sci USA.* 1998;95:15792-7.
- [23] Bhattacharya M, Peri K, Ribeiro-da-Silva A, Almazan G, Shichi H, Hou X, et al. Localization of functional prostaglandin E2 receptors EP3 and EP4 in the nuclear envelope. *J Biol Chem.* 1999;274:15719-24.
- [24] Gobeil F, Jr., Dumont I, Marrache AM, Vazquez-Tello A, Bernier SG, Abran D, et al. Regulation of eNOS expression in brain endothelial cells by perinuclear EP<sub>3</sub> receptors. *Circ Res.* 2002;90:682-9.

- [25] Gobeil F, Jr., Bernier SG, Vazquez-Tello A, Brault S, Beauchamp MH, Quiniou C, et al. Modulation of pro-inflammatory gene expression by nuclear lysophosphatidic acid receptor type-1. *J Biol Chem.* 2003;278:38875-83.
- [26] Gobeil F, Jr., Zhu T, Brault S, Geha A, Vazquez-Tello A, Fortier A, et al. Nitric oxide signaling via nuclearized endothelial nitric-oxide synthase modulates expression of the immediate early genes iNOS and mPGES-1. *J Biol Chem.* 2006;281:16058-67.
- [27] Jong YJ, Kumar V, O'Malley KL. Intracellular metabotropic glutamate receptor 5 (mGluR5) activates signaling cascades distinct from cell surface counterparts. *J Biol Chem.* 2009;284:35827-38.
- [28] Kumar V, Fahey PG, Jong YJ, Ramanan N, O'Malley KL. Activation of intracellular metabotropic glutamate receptor 5 in striatal neurons leads to up-regulation of genes associated with sustained synaptic transmission including Arc/Arg3.1 protein. *J Biol Chem.* 2012;287:5412-25.
- [29] Ramamurthy S, Mir F, Gould RM, Le Breton GC. Characterization of thromboxane A2 receptor signaling in developing rat oligodendrocytes: nuclear receptor localization and stimulation of myelin basic protein expression. *J Neurosci Res.* 2006;84:1402-14.
- [30] Mir F, Le Breton GC. A novel nuclear signaling pathway for thromboxane A2 receptors in oligodendrocytes: evidence for signaling compartmentalization during differentiation. *Mol Cell Biol.* 2008;28:6329-41.
- [31] Nguyen TT, Letourneau M, Chatenet D, Fournier A. Presence of urotensin-II receptors at the cell nucleus: specific tissue distribution and hypoxia-induced modulation. *Int J Biochem Cell Biol.* 2012;44:639-47.

- [32] Chevalier D, Allen BG. Two distinct forms of MAPKAP kinase-2 in adult cardiac ventricular myocytes. *Biochemistry*. 2000;39:6145-56.
- [33] Jackowski G, Liew CC. Fractionation of rat ventricular nuclei. *Biochem J*. 1980;188:363-73.
- [34] Ventura C, Pintus G, Vaona I, Bennardini F, Pinna G, Tadolini B. Phorbol ester regulation of opioid peptide gene expression in myocardial cells. Role of nuclear protein kinase. *J Biol Chem*. 1995;270:30115-20.
- [35] Thorin E, Shatos MA, Shreeve SM, Walters CL, Bevan JA. Human vascular endothelium heterogeneity. A comparative study of cerebral and peripheral cultured vascular endothelial cells. *Stroke*. 1997;28:375-81.
- [36] Thorin E, Hamilton C, Dominiczak AF, Reid JL. Chronic exposure of cultured bovine endothelial cells to oxidized low density lipoprotein abolished prostacyclin release. *Arterioscler Thromb*. 1994;14:453-9.
- [37] Bourgault S, Létourneau M, Fournier A. Development of photolabile caged analogs of endothelin-1. *Peptides*. 2007;28:1074-82.
- [38] Allen BG, Farhat H, Phuong LL, Chevalier D. Both endothelin-A and endothelin-B receptors are present on adult rat cardiac ventricular myocytes. *Can J Physiol Pharmacol*. 2003;81:95-104.
- [39] Farih J, Touyz RM, Schiffrin EL, Thibault G. Endothelin-1 and angiotensin II receptors in cells from rat hypertrophied heart. Receptor regulation and intracellular Ca<sup>2+</sup> modulation. *Circ Res*. 1996;78:302-11.

- [40] Oksche A, Boese G, Horstmeyer A, Furkert J, Beyermann M, Bienert M, et al. Late endosomal/lysosomal targeting and lack of recycling of the ligand-occupied endothelin B receptor. *Mol Pharmacol.* 2000;57:1104-13.
- [41] Waggoner WG, Genova SL, Rash VA. Kinetic analyses demonstrate that the equilibrium assumption does not apply [<sup>125</sup>I]endothelin-1 binding data. *Life Sci.* 1992;51:1869-76.
- [42] Gregan B, Jurgensen J, Papsdorf G, Furkert J, Schaefer M, Beyermann M, et al. Ligand-dependent differences in the internalization of endothelin A and endothelin B receptor heterodimers. *J Biol Chem.* 2004;279:27679-87.
- [43] Harada N, Himeno A, Shigematsu K, Sumikawa K, Niwa M. Endothelin-1 binding to endothelin receptors in the rat anterior pituitary gland: possible formation of an ETA-ETB receptor heterodimer. *Cell Mol Neurobiol.* 2002;22:207-26.
- [44] Lee DK, Lanca AJ, Cheng R, Nguyen T, Ji XD, Gobeil F, Jr., et al. Agonist-independent nuclear localization of the Apelin, angiotensin AT1, and bradykinin B2 receptors. *J Biol Chem.* 2004;279:7901-8.
- [45] Watson PH, Pickard BW. Nuclear trafficking of the G-protein-coupled parathyroid hormone receptor. *Crit Rev Eukaryot Gene Expr.* 2008;18:151-61.
- [46] Goldfarb DS, Corbett AH, Mason DA, Harreman MT, Adam SA. Importin  $\alpha$ : a multipurpose nuclear-transport receptor. *Trends Cell Biol.* 2004;14:505-14.
- [47] Bousso-Mittler D, Galron R, Sokolovsky M. Endothelin/sarafotoxin receptor heterogeneity: evidence for different glycosylation in receptors from different tissues. *Biochem Biophys Res Commun.* 1991;178:921-6.
- [48] Sokolovsky M, Ambar I, Galron R. A novel subtype of endothelin receptors. *J Biol Chem.* 1992;267:20551-4.

- [49] Wu X, Zhang T, Bossuyt J, Li X, McKinsey TA, Dedman JR, et al. Local  $\text{InsP}_3$ -dependent perinuclear  $\text{Ca}^{2+}$  signaling in cardiac myocyte excitation-transcription coupling. *J Clin Invest.* 2006;116:675-82.
- [50] Takahashi A, Camacho P, Lechleiter JD, Herman B. Measurement of intracellular calcium. *Physiol Rev.* 1999;79:1089-125.
- [51] Thomas D, Tovey SC, Collins TJ, Bootman MD, Berridge MJ, Lipp P. A comparison of fluorescent  $\text{Ca}^{2+}$  indicator properties and their use in measuring elementary and global  $\text{Ca}^{2+}$  signals. *Cell Calcium.* 2000;28:213-23.
- [52] Wu X, Bers DM. Sarcoplasmic reticulum and nuclear envelope are one highly interconnected  $\text{Ca}^{2+}$  store throughout cardiac myocyte. *Circ Res.* 2006;99:283-91.
- [53] Hansford RG, Lakatta EG. Ryanodine releases calcium from sarcoplasmic reticulum in calcium-tolerant rat cardiac myocytes. *J Physiol.* 1987;390:453-67.
- [54] Bare DJ, Kettlun CS, Liang M, Bers DM, Mignery GA. Cardiac type 2 inositol 1,4,5-trisphosphate receptor. Interaction and modulation by calcium/calmodulin-dependent protein kinase II. *J Biol Chem.* 2005;280:15912-020.
- [55] Abadir PM, Foster DB, Crow M, Cooke CA, Rucker JJ, Jain A, et al. Identification and characterization of a functional mitochondrial angiotensin system. *Proc Natl Acad Sci U S A.* 2011;108:14849-54.
- [56] Hocher B, Rubens C, Hensen J, Gross P, Bauer C. Intracellular distribution of endothelin-1 receptors in rat liver cells. *Biochem Biophys Res Commun.* 1992;184:498-503.
- [57] Liu T, Long L, Tang T, Xia Q, Liu J, He G, et al. Expression and localization of endothelin-1 and its receptors in the spiral ganglion neurons of mouse. *Cell Mol Neurobiol.* 2009;29:739-45.

- [58] Chun M, Lin HY, Henis YI, Lodish HF. Endothelin-induced endocytosis of cell surface ET<sub>A</sub> receptors. Endothelin remains intact and bound to the ET<sub>A</sub> receptor. *J Biol Chem.* 1995;270:10855-60.
- [59] Wright CD, Wu SC, Dahl EF, Sazama AJ, O'Connell TD. Nuclear localization drives  $\alpha$ 1-adrenergic receptor oligomerization and signaling in cardiac myocytes. *Cell Signal.* 2012;24:794-802.
- [60] Wright CD, Chen Q, Baye NL, Huang Y, Healy CL, Kasinathan S, et al. Nuclear  $\alpha$ 1-adrenergic receptors signal activated ERK localization to caveolae in adult cardiac myocytes. *Circ Res.* 2008;103:992-1000.
- [61] Grantcharova E, Furkert J, Reusch HP, Krell H-W, Papsdorf G, Beyermann M, et al. The extracellular N terminal of the endothelin B (ET<sub>B</sub>) receptor is cleaved by a metalloprotease in an agonist-dependent process. *J Biol Chem.* 2002;277:43933-41.
- [62] Carey RM. Functional intracellular renin-angiotensin systems: potential for pathophysiology of disease. *Am J Physiol Regul Integr Comp Physiol.* 2012;302:R479-R81.
- [63] Cook JL, Re RN. Lessons from in vitro studies and a related intracellular angiotensin II transgenic mouse model. *Am J Physiol Regul Integr Comp Physiol.* 2012;302:R482-R93.
- [64] Ellis B, Li XC, Miguel-Qin E, Gu V, Zhuo JL. Evidence for a functional intracellular angiotensin system in the proximal tubule of the kidney. *Am J Physiol Regul Integr Comp Physiol.* 2012;302:R494-R509.
- [65] Gwathmey TM, Alzayadneh EM, Pendergrass KD, Chappell MC. Novel roles of nuclear angiotensin receptors and signaling mechanisms. *Am J Physiol Regul Integr Comp Physiol.* 2012;302:R518-R30.

- [66] Re RN, Cook JL. Noncanonical intracrine action. *J Am Soc Hypertens.* 2011;5:435-48.
- [67] Zhuo JL, Li XC. New insights and perspectives on intrarenal renin-angiotensin system: focus on intracrine/intracellular angiotensin II. *Peptides.* 2011;32:1551-65.
- [68] Ergul A, Walker CA, Goldberg A, Baicu SC, Hendrick JW, King MK, et al. ET-1 in the myocardial interstitium: relation to myocyte ECE activity and expression. *Am J Physiol.* 2000;278:H2050-H6.
- [69] Jafri F, Ergul A. Nuclear localization of endothelin-converting enzyme-1. Subisoform specificity. *Arterioscler Thromb Vasc Biol.* 2003;23:2192-6.
- [70] Hunter AR, Turner AJ. Expression and localization of endothelin-converting enzyme-1 isoforms in human endothelial cells. *Exp Biol Med.* 2006;231:718-22.
- [71] Suzuki T, Kumazaki T, Mitsui Y. Endothelin-1 is produced and secreted by neonatal rat cardiac myocytes *in vitro*. *Biochem Biophys Res Commun.* 1993;191:823-30.
- [72] Thomas PB, Liu EDK, Webb ML, Mukherjee R, Hebbar L, Spinale FG. Exogenous effects and endogenous production of endothelin in cardiac myocytes: potential significance in heart failure. *Am J Physiol.* 1996;271:H2629-H37.
- [73] Yamazaki T, Komuro I, Kudoh S, Zou YZ, Shiojima I, Hiroi Y, et al. Endothelin-1 is involved in mechanical stress-induced cardiomyocyte hypertrophy. *J Biol Chem.* 1996;271:3221-8.
- [74] Farhat N, Matouk CC, Mamarbachi AM, Marsden PA, Allen BG, Thorin E. Activation of ET<sub>B</sub> receptors regulates the abundance of ET-1 mRNA in vascular endothelial cells. *Br J Pharmacol.* 2008;153:1420-31.

- [75] Kedzierski RM, Yanagisawa M. Endothelin system: the double-edged sword in health and disease. *Annu Rev Pharmacol Toxicol.* 2001;41:851-76.
- [76] Mawji IA, Marsden PA. Perturbations in paracrine control of the circulation: role of the endothelial-derived vasomediators, endothelin-1 and nitric oxide. *Microsc Res Tech.* 2003;60:46-58.
- [77] Morimoto T, Hasegawa K, Wada H, Kakita T, Kaburagi S, Yanazume T, et al. Calcineurin-GATA4 pathway is involved in  $\beta$ -adrenergic agonist-responsive endothelin-1 transcription in cardiac myocytes. *J Biol Chem.* 2001;276:34983-9.
- [78] Booz GW, Conrad KM, Hess AL, Singer HA, Baker KM. Angiotensin-II binding sites on hepatocyte nuclei. *Endocrinology.* 1992;130:3641-9.
- [79] Cook JL, Mills SJ, Naquin R, Alam J, Re RN. Nuclear accumulation of the AT1 receptor in a rat vascular smooth muscle cell line: effects upon signal transduction and cellular proliferation. *J Mol Cell Cardiol.* 2006;40:696-707.
- [80] Dostal DE, Rothblum KN, Conrad KM, Cooper GR, Baker KM. Detection of angiotensin I and II in cultured rat cardiac myocytes and fibroblasts. *Am J Physiol.* 1992;263:C851-C63.
- [81] Camargo de Andrade MC, Di Marco GS, de Paulo Castro Teixeira V, Mortara RA, Sabatini RA, Pesquero JB, et al. Expression and localization of N-domain ANG I-converting enzymes in mesangial cells in culture from spontaneously hypertensive rats. *Am J Physiol Renal Physiol.* 2006;290:F364-F75.
- [82] Frustaci A, Kajstura J, Chimenti C, Jakoniuk I, Leri A, Maseri A, et al. Myocardial cell death in human diabetes. *Circ Res.* 2000;87:1123-32.

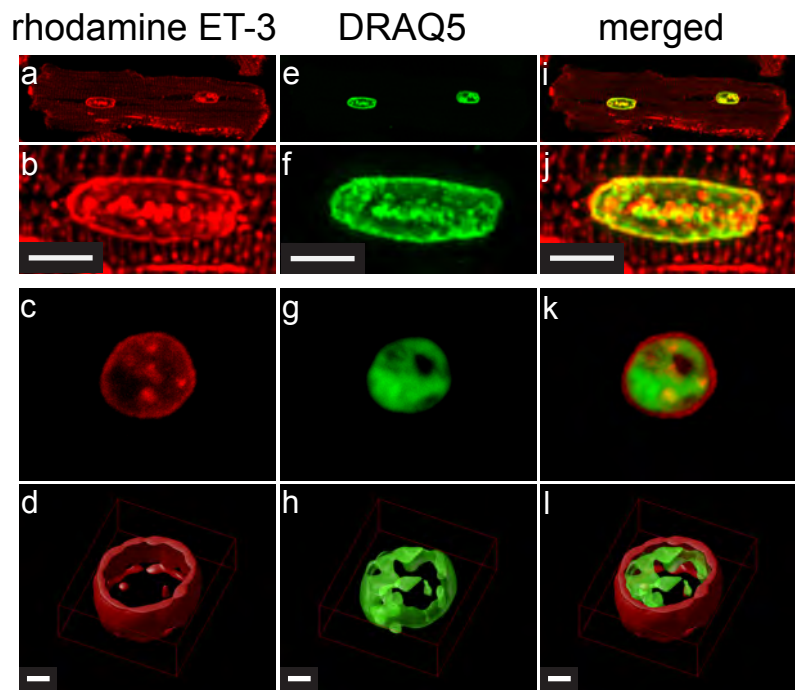
- [83] Baker KM, Chernin MI, Schreiber T, Sanghi S, Haiderzaidi S, Booz GW, et al. Evidence of a novel intracrine mechanism in angiotensin II-induced cardiac hypertrophy. *Regul Pept.* 2004;120:5-13.
- [84] Mazzolai L, Nussberger J, Aubert JF, Brunner DB, Gabbiani G, Brunner HR, et al. Blood pressure-independent cardiac hypertrophy induced by locally activated renin-angiotensin system. *Hypertension.* 1998;31:1324-30.
- [85] Remus TP, Zima AV, Bossuyt J, Bare DJ, Martin JL, Blatter LA, et al. Biosensors to measure inositol 1,4,5-trisphosphate concentration in living cells with spatiotemporal resolution. *J Biol Chem.* 2006;281:608-16.
- [86] Zima AV, Bare DJ, Mignery GA, Blatter LA. IP<sub>3</sub>-dependent nuclear Ca<sup>2+</sup> signalling in the mammalian heart. *J Physiol.* 2007;584:601-11.
- [87] Kockskamper J, Seidlmayer L, Walther S, Hellenkamp K, Maier LS, Pieske B. Endothelin-1 enhances nuclear Ca<sup>2+</sup> transients in atrial myocytes through Ins(1,4,5)P<sub>3</sub>-dependent Ca<sup>2+</sup> release from perinuclear Ca<sup>2+</sup> stores. *J Cell Sci.* 2008;121:186-95.
- [88] Bkaily G, Pothier P, D'Orleans-Juste P, Simaan M, Jacques D, Jaalouk D, et al. The use of confocal microscopy in the investigation of cell structure and function in the heart, vascular endothelium and smooth muscle cells. *Mol Cell Biochem.* 1997;172:171-94.
- [89] Bkaily G, Nader M, Avedanian L, Choufani S, Jacques D, D'Orleans-Juste P, et al. G-protein-coupled receptors, channels, and Na<sup>+</sup>-H<sup>+</sup> exchanger in nuclear membranes of heart, hepatic, vascular endothelial, and smooth muscle cells. *Can J Physiol Pharmacol.* 2006;84:431-41.
- [90] Bootman MD, Fearnley C, Smyrniak I, MacDonald F, Roderick HL. An update on nuclear calcium signalling. *J Cell Sci.* 2009;122:2337-50.

- [91] Zhuo JL, Li XC, Garvin JL, Navar LG, Carretero OA. Intracellular ANG II induces cytosolic Ca<sup>2+</sup> mobilization by stimulating intracellular AT1 receptors in proximal tubule cells. *Am J Physiol Renal Physiol*. 2006;290:F1382-F90.
- [92] Jong YJ, Kumar V, Kingston AE, Romano C, O'Malley KL. Functional metabotropic glutamate receptors on nuclei from brain and primary cultured striatal neurons. Role of transporters in delivering ligand. *J Biol Chem*. 2005;280:30469-80.
- [93] Jong YJ, Schwetye KE, O'Malley KL. Nuclear localization of functional metabotropic glutamate receptor mGlu1 in HEK293 cells and cortical neurons: role in nuclear calcium mobilization and development. *J Neurochem*. 2007;101:458-69.
- [94] Kumar V, Jong YJ, O'Malley KL. Activated nuclear metabotropic glutamate receptor mGlu5 couples to nuclear Gq/11 proteins to generate inositol 1,4,5-trisphosphate-mediated nuclear Ca<sup>2+</sup> release. *J Biol Chem*. 2008;283:14072-83.
- [95] O'Malley KL, Jong YJ, Gonchar Y, Burkhalter A, Romano C. Activation of metabotropic glutamate receptor mGlu5 on nuclear membranes mediates intranuclear Ca<sup>2+</sup> changes in heterologous cell types and neurons. *J Biol Chem*. 2003;278:28210-9.
- [96] Nakayama H, Bodi I, Maillet M, DeSantiago J, Domeier TL, Mikoshiba K, et al. The IP<sub>3</sub> receptor regulates cardiac hypertrophy in response to select stimuli. *Circ Res*. 2010;107:659-66.
- [97] Uwada J, Anisuzzaman AS, Nishimune A, Yoshiki H, Muramatsu I. Intracellular distribution of functional M<sub>1</sub> -muscarinic acetylcholine receptors in N1E-115 neuroblastoma cells. *J Neurochem*. 2011;118:958-67.
- [98] Ryall KA, Saucerman JJ. Automated imaging reveals a concentration dependent delay in reversibility of cardiac myocyte hypertrophy. *J Mol Cell Cardiol*. 2012;53:282-90.

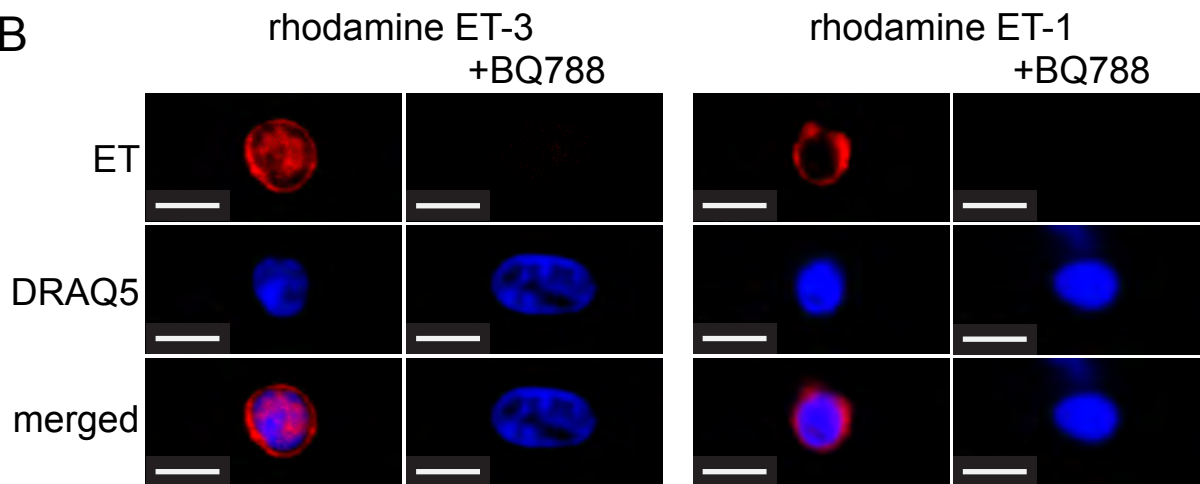
- [99] Bootman MD, Collins TJ, Mackenzie L, Roderick HL, Berridge MJ, Peppiatt CM. 2-aminoethoxydiphenyl borate (2-APB) is a reliable blocker of store-operated  $\text{Ca}^{2+}$  entry but an inconsistent inhibitor of  $\text{InsP}_3$ -induced  $\text{Ca}^{2+}$  release. *FASEB J.* 2002;16:1145-50.
- [100] Peppiatt CM, Collins TJ, Mackenzie L, Conway SJ, Holmes AB, Bootman MD, et al. 2-Aminoethoxydiphenyl borate (2-APB) antagonises inositol 1,4,5-trisphosphate-induced calcium release, inhibits calcium pumps and has a use-dependent and slowly reversible action on store-operated calcium entry channels. *Cell Calcium.* 2003;34:97-108.
- [101] DeHaven WI, Smyth JT, Boyles RR, Bird GS, Putney JW, Jr. Complex actions of 2-aminoethoxydiphenyl borate on store-operated calcium entry. *J Biol Chem.* 2008;283:19265-73.

Figure 1

A



B



C

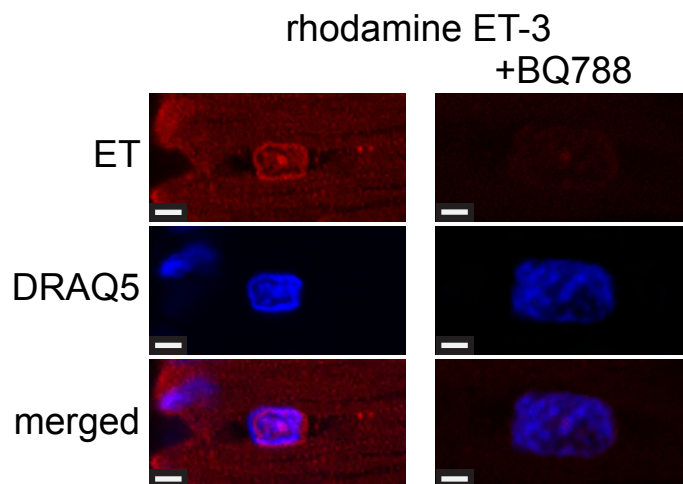


Figure 2

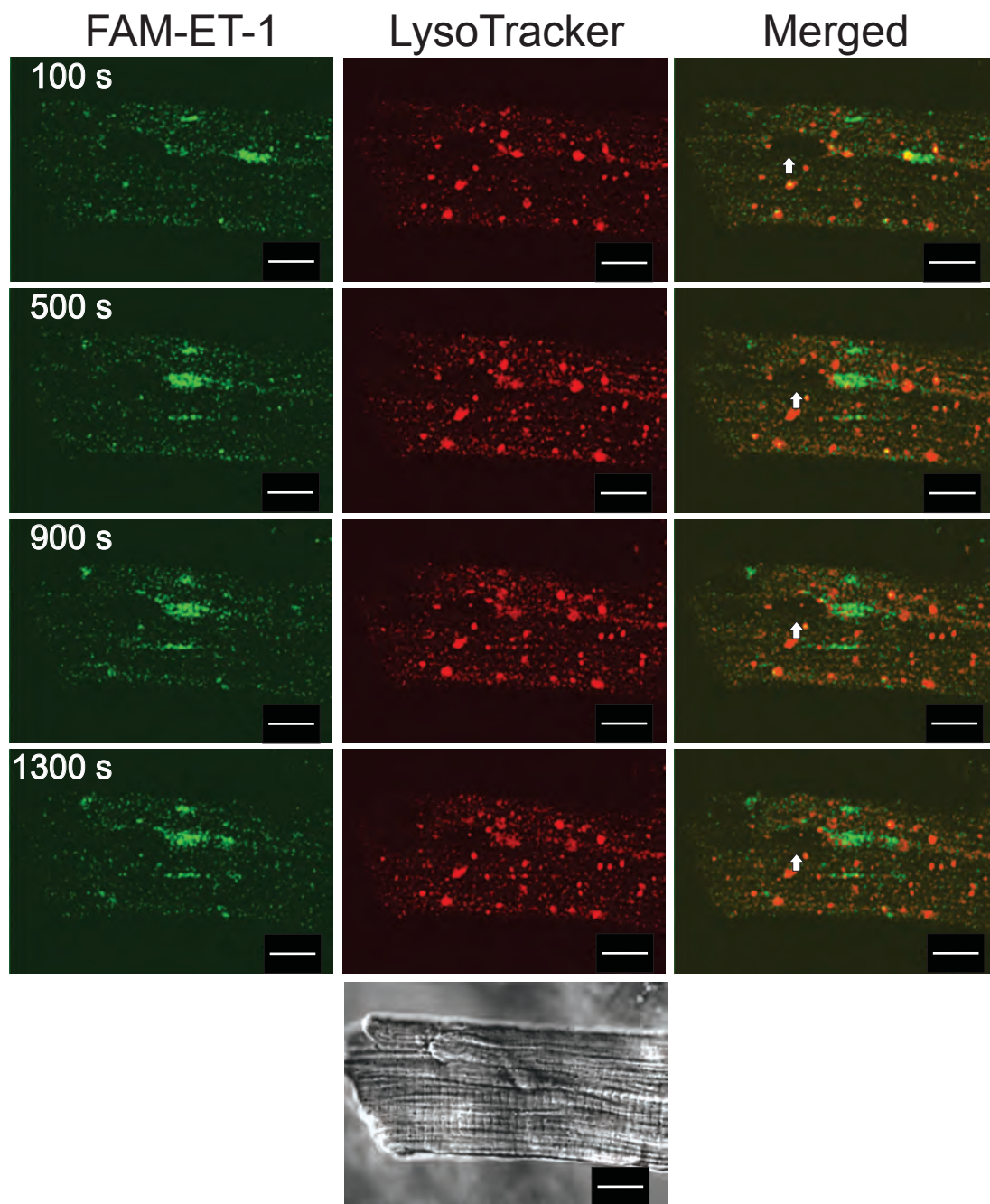


Figure 3

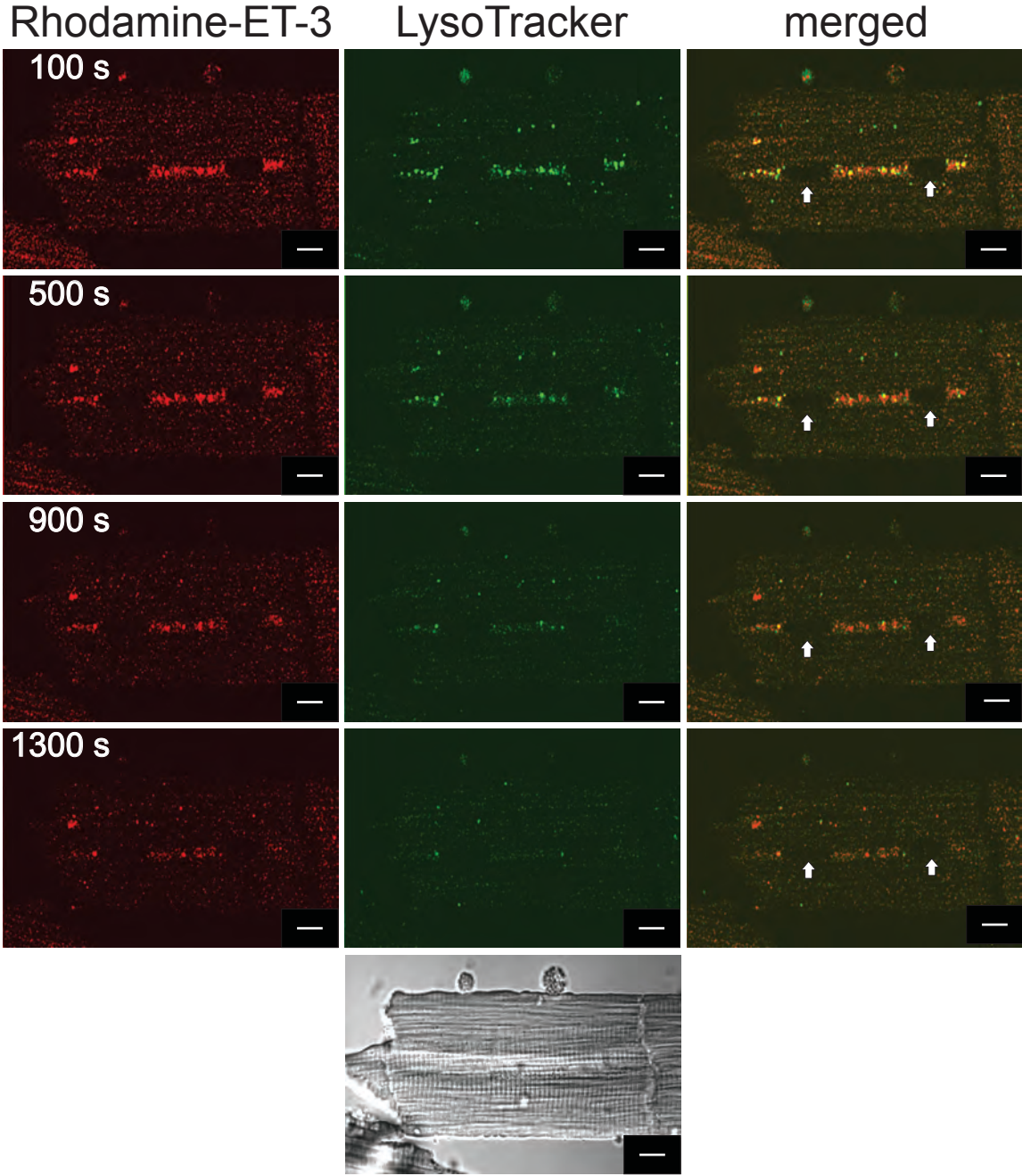


Figure 4

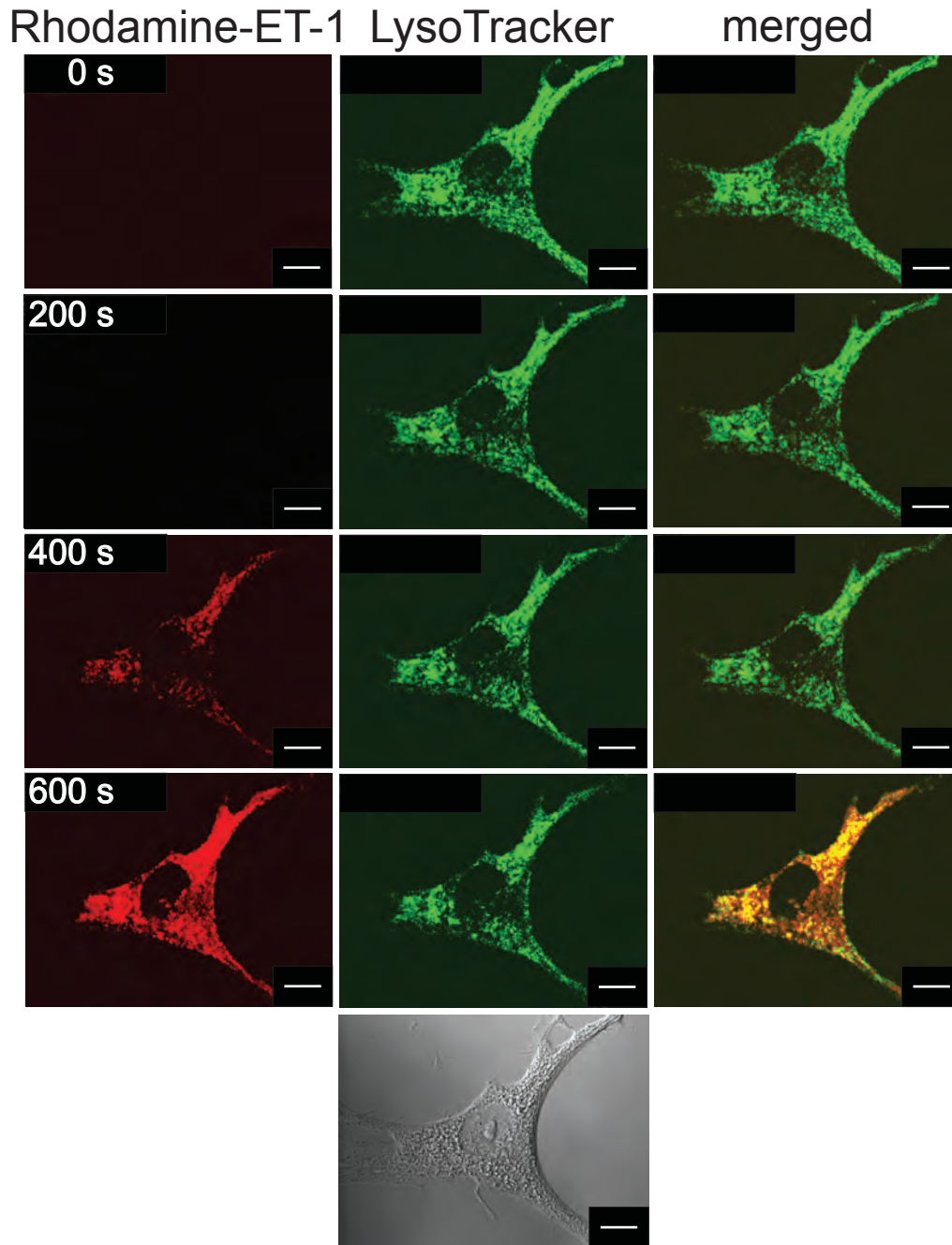
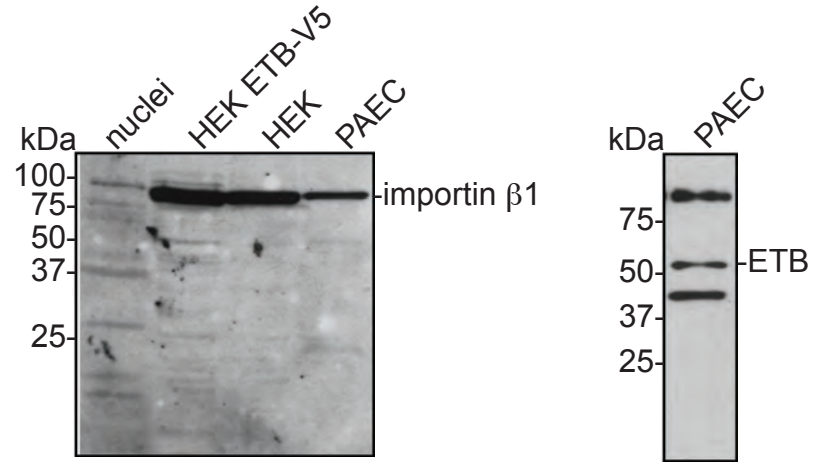
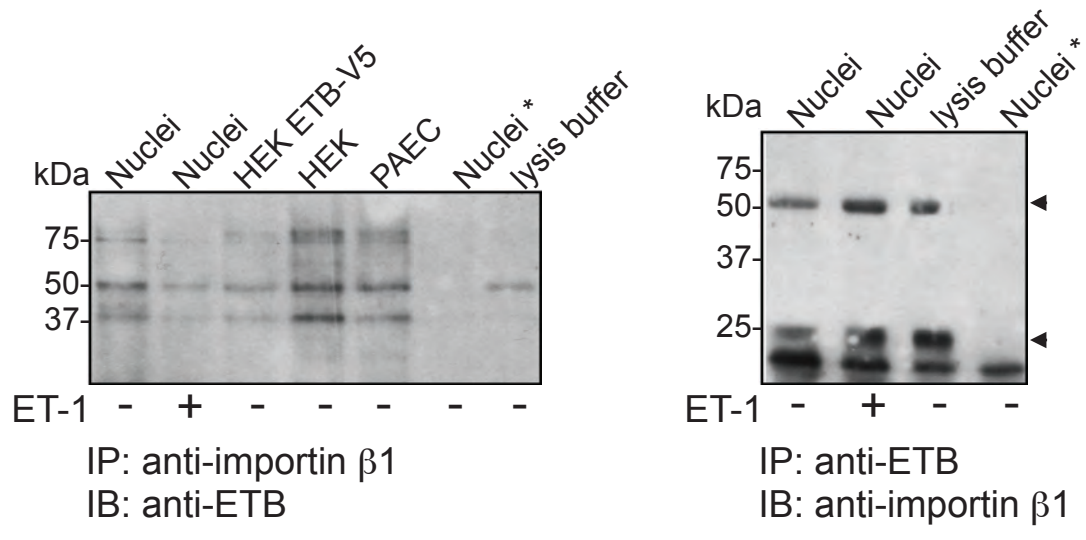


Figure 5

**A**



**B**



**C**

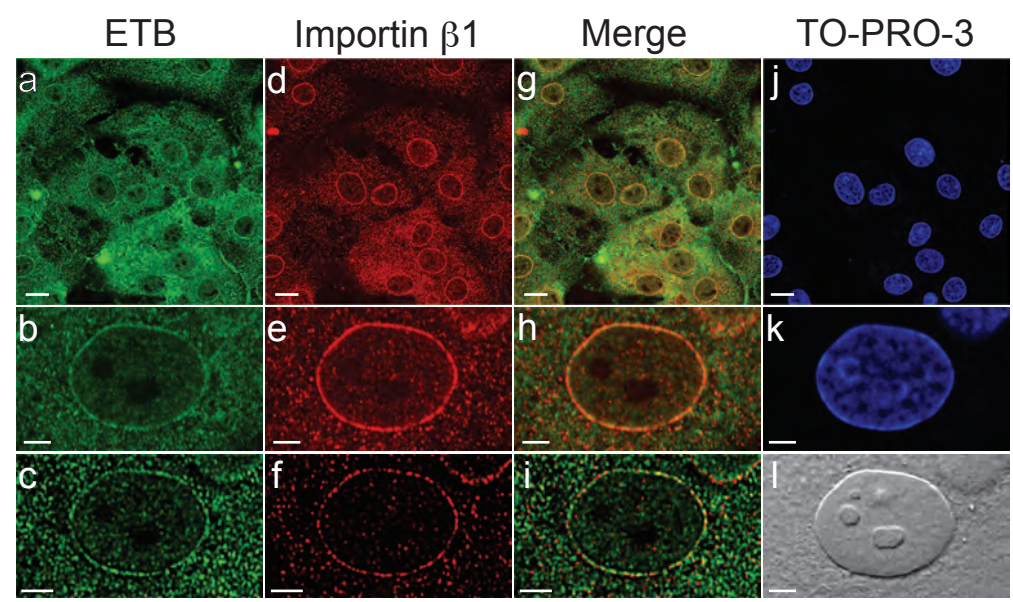
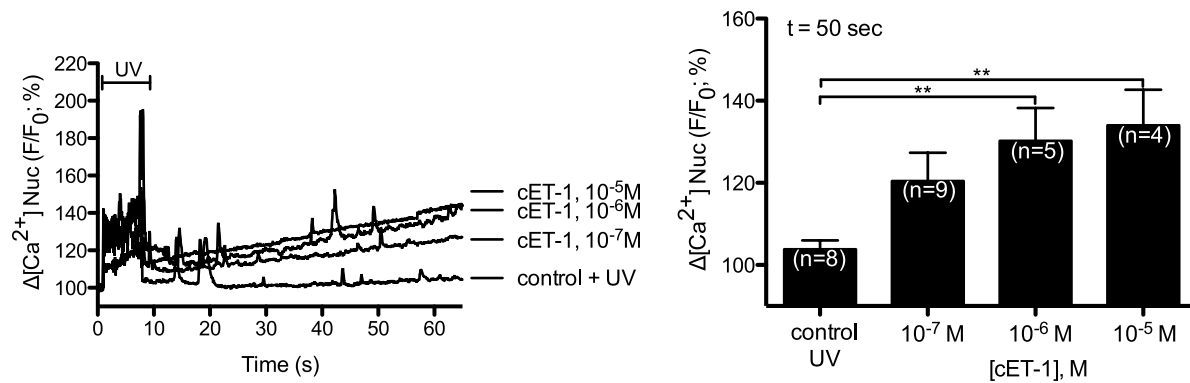


Figure 6

A



B

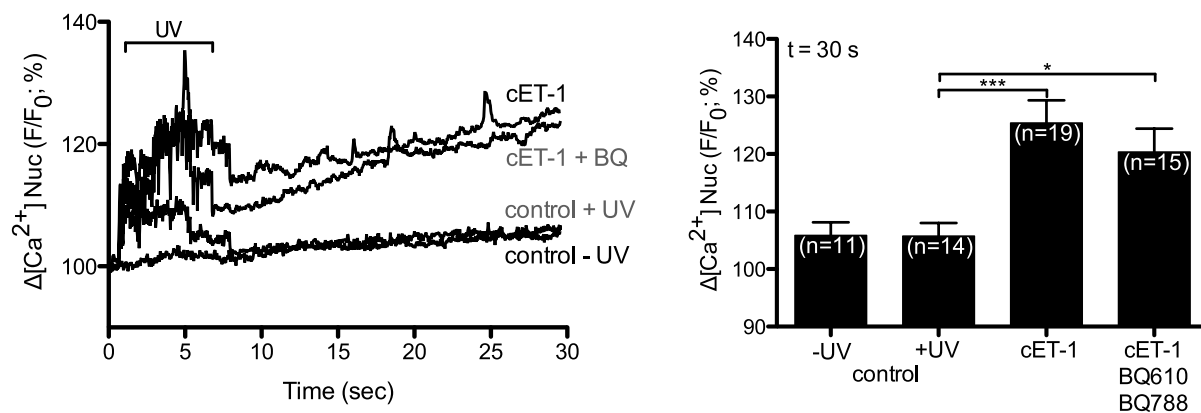
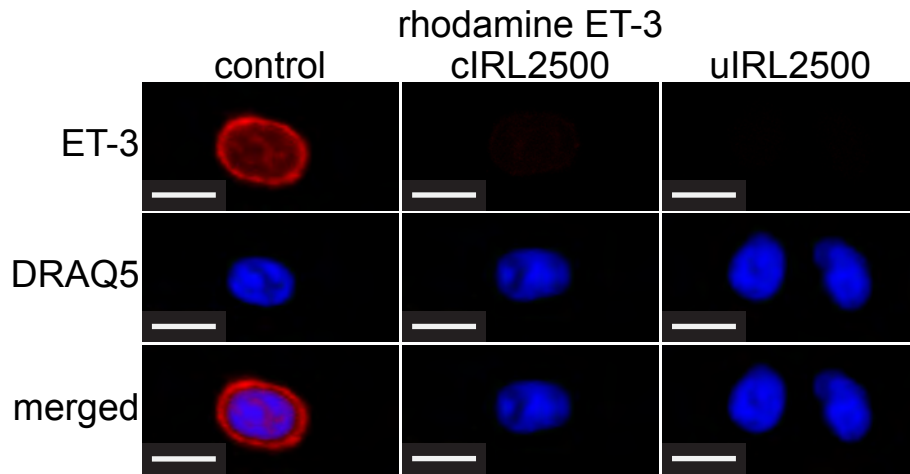


Figure 7

A



B

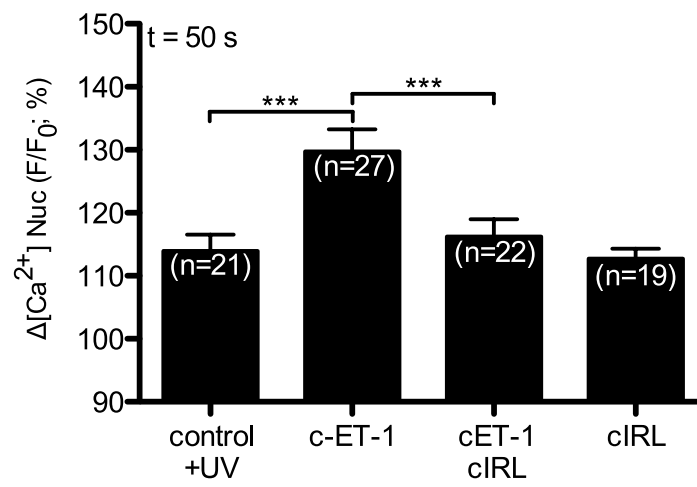
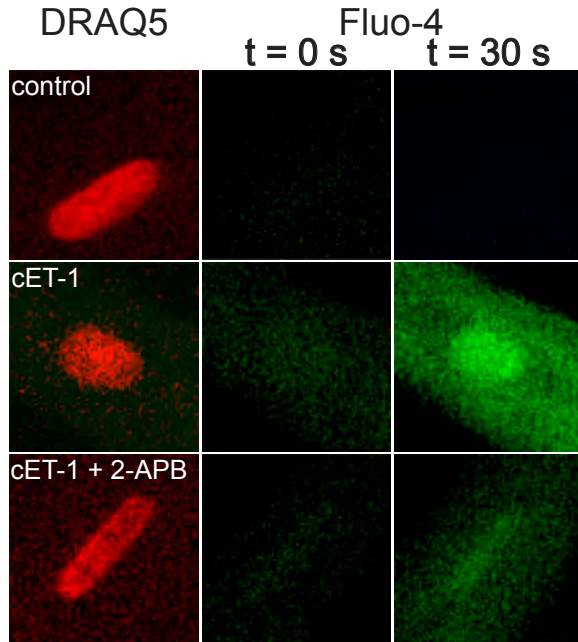
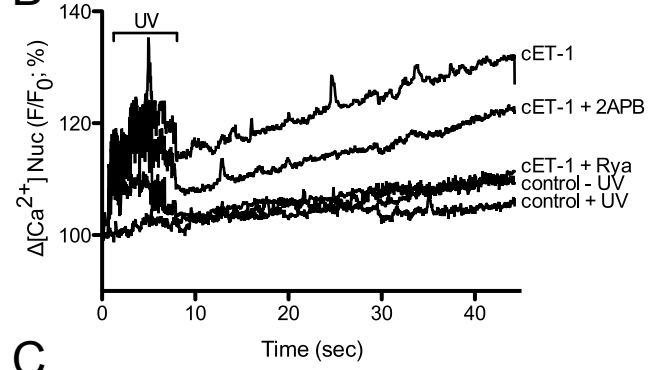


Figure 8

A



B



C

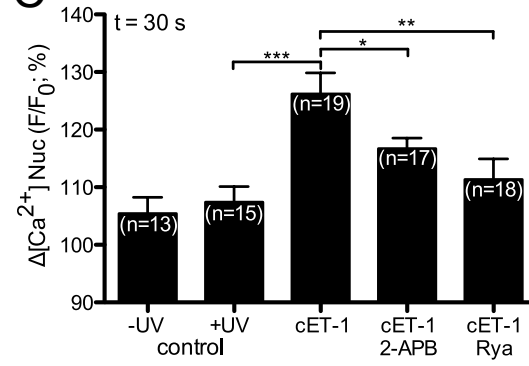
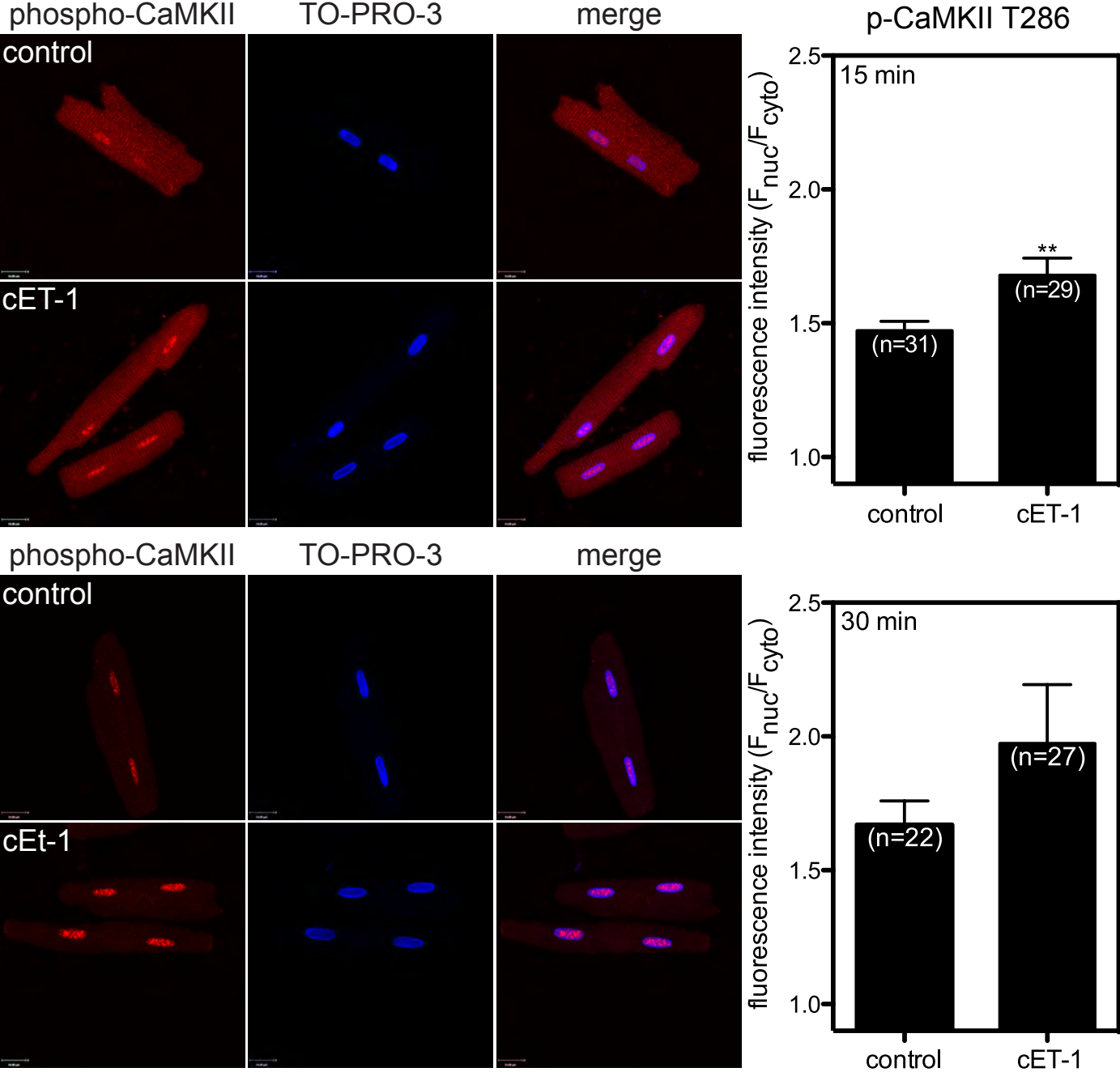


Figure 9



**Supplemental Table 1. The primers used for qPCR**

| Target   | Primers                          |
|----------|----------------------------------|
| ET-1 S   | 5'-GAC CAG CGT CCT TGT TCC AA-3' |
| ET-1 AS  | 5'-TTG CTA CCA GCG GAT GCA A-3'  |
| GAPDH S  | 5'-TGC CCC CAT GTT TGT GAT G-3'  |
| GAPDH AS | 5'-GTG GTG CAG GAT GCA TTG C-3'  |

S, sense; AS, anti-sense; GAPDH, glyceraldehyde 3-phosphate dehydrogenase; qPCR, quantitative polymerase chain reaction.

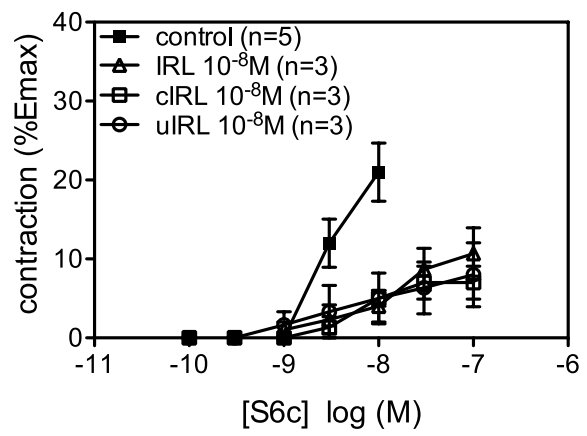
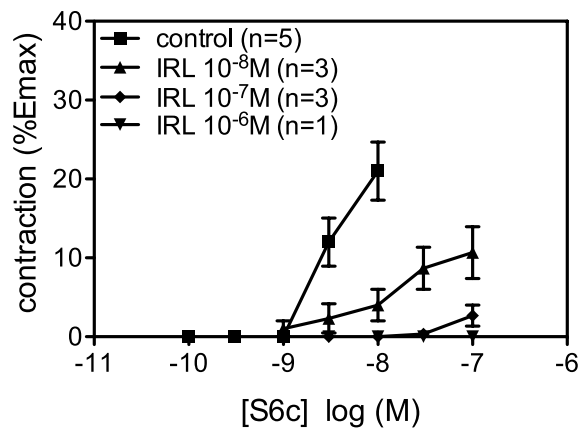
## **Supplemental Figure Legends**

**Supplemental Figure 1. Caged IRL2500 retains its ability to antagonize ligand binding to ETB.** Mouse tracheal rings (1 mm) were mounted on a wire myograph and a preload of 1 g was applied. The ETB-selective agonist sarafotoxin 6c (S6c) was added cumulatively in the presence or absence of IRL2500. Concentration-response curves were performed in the presence of the indicated concentrations of IRL2500 (IRL; left panel) or 10 nM (right panel) of either unmodified IRL2500 (IRL), caged IRL2500 (cIRL), or photolysed, caged IRL2500 (uIRL). The contractile response is presented as a percentage of the contraction induced by KCl. Each point represents the mean  $\pm$  SE.

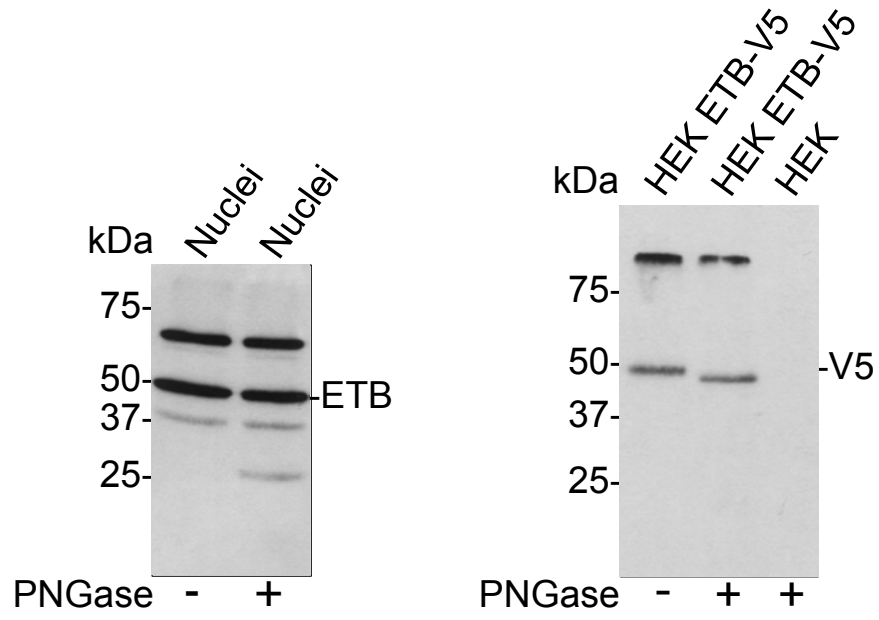
**Supplemental Figure 2. Deglycosylation of ETB.** Nuclei isolated from rat heart were incubated with PNGase F at 37 °C for 5 h (left panel). As a positive control, HEK293 cells expressing ETB-V5 were similarly treated (right panel). ETB was then visualized by immunoblot analysis using anti-ETB (left) or anti-V5 (right) antibodies. Numbers to the left indicate the positions of the prestained molecular mass markers proteins (in kDa).

**Supplemental Figure 3. Adult cardiac ventricular myocytes express ET-1 and extracellular ET-1 suppresses intracellular ET-1 mRNA levels via ETA.** Freshly isolated adult rat ventricular myocytes were incubated for 4 h in buffer containing vehicle (DMSO) or with ET-1 (10 nM), ET-1 plus BQ610 (ETA antagonist, 1  $\mu$ M), ET-1 plus BQ788 (ETB antagonist, 1  $\mu$ M), or ET-1 plus BQ610 and BQ788. ET-1 and GAPDH mRNA were quantified by qPCR. Single amplicons were obtained and verified by sequencing. Results are means  $\pm$  s.e.m. of separate experiments employing 4 or 6 (control, ET-1) different myocyte preparations. \*\*,  $p < 0.01$  versus control (one-way ANOVA, Dunnett's Multiple Comparison post-tests). Primers used in qPCR are listed in Supplemental Table 1.

Supplemental Figure 1



Supplemental Figure 2



Supplemental Figure 3

